

NAVAL POSTGRADUATE SCHOOL

Monterey, California



THESIS

VALUE AIDED SATELLITE ALTIMETRY DATA FOR WEAPON PRESETS

by

Michael D. Perry

June 2003

Thesis Advisor:
Second Reader:

Peter Chu
Eric Gottshall

Approved for public release; distribution is unlimited

THIS PAGE INTENTIONALLY LEFT BLANK

| | | | | |
|--|---|--|--|--|
| REPORT DOCUMENTATION PAGE | | | <i>Form Approved OMB No. 0704-0188</i> | |
| Public reporting burden for this collection of information is estimated to average 1 hour per response, including the time for reviewing instruction, searching existing data sources, gathering and maintaining the data needed, and completing and reviewing the collection of information. Send comments regarding this burden estimate or any other aspect of this collection of information, including suggestions for reducing this burden, to Washington headquarters Services, Directorate for Information Operations and Reports, 1215 Jefferson Davis Highway, Suite 1204, Arlington, VA 22202-4302, and to the Office of Management and Budget, Paperwork Reduction Project (0704-0188) Washington DC 20503. | | | | |
| 1. AGENCY USE ONLY (Leave blank) | | 2. REPORT DATE June 2003 | 3. REPORT TYPE AND DATES COVERED Master's Thesis | |
| 4. TITLE AND SUBTITLE: Title (Mix case letters) Value Aided Satellite Altimetry Data for Weapon Presets | | | 5. FUNDING NUMBERS N0003902WRHK502 | |
| 6. AUTHOR(S) Michael Perry | | | | |
| 7. PERFORMING ORGANIZATION NAME(S) AND ADDRESS(ES) Naval Postgraduate School Monterey, CA 93943-5000 | | | 8. PERFORMING ORGANIZATION REPORT NUMBER | |
| 9. SPONSORING /MONITORING AGENCY NAME(S) AND ADDRESS(ES) CDR Eric Gottshall, SPAWAR PMW-155 4301 Pacific Highway, OT-1, Rm 1187 San Diego, CA 92110-3127 | | | 10. SPONSORING/MONITORING AGENCY REPORT NUMBER | |
| 11. SUPPLEMENTARY NOTES The views expressed in this thesis are those of the author and do not reflect the official policy or position of the Department of Defense or the U.S. Government. | | | | |
| 12a. DISTRIBUTION / AVAILABILITY STATEMENT Approved for public release; distribution is unlimited | | | 12b. DISTRIBUTION CODE | |
| 13. ABSTRACT (maximum 200 words) The purpose of this thesis is to determine the effect that the inclusion of satellite altimeter data has on weapon preset accuracy. GDEM data and MODAS data utilizing four satellite altimeters were used by the Weapon Acoustic Preset Program to determine the suggested presets for a Mk 48 torpedo. The acoustic coverage area generated by the program will be used as the metric to compare the two sets of outputs. The assumption is that the MODAS initialized presets will be more accurate, and, therefore, the difference between the two sets of presets can be attributed to inaccuracy on the part of the GDEM presets. Output presets were created for two different scenarios, an Anti-Surface Warfare (ASUW) scenario and an Anti-Submarine Warfare (ASW) scenario, and three different depth bands, shallow, mid, and deep. After analyzing the output, it became clear that the GDEM data predicted a weapon effectiveness that was far higher than the effectiveness predicted by the MODAS data. Also, while GDEM predicted a wide range of coverage percentages MODAS predicted a narrow range of coverage percentages. | | | | |
| 14. SUBJECT TERMS GDEM, MODAS, Mk 48, satellite altimeter, temperature, salinity, sound speed profile, ray trace, signal excess, ASW, ASUW | | | 15. NUMBER OF PAGES 86 | |
| | | | 16. PRICE CODE | |
| 17. SECURITY CLASSIFICATION OF REPORT Unclassified | 18. SECURITY CLASSIFICATION OF THIS PAGE Unclassified | 19. SECURITY CLASSIFICATION OF ABSTRACT Unclassified | 20. LIMITATION OF ABSTRACT UL | |

NSN 7540-01-280-5500

Standard Form 298 (Rev. 2-89)
Prescribed by ANSI Std. Z39-18

THIS PAGE INTENTIONALLY LEFT BLANK

Approved for public release; distribution is unlimited

VALUE AIDED SATELLITE ALTIMETRY DATA FOR WEAPON PRESETS

Michael D. Perry
Ensign, United States Navy
B.S., Auburn University, 2002

Submitted in partial fulfillment of the
requirements for the degree of

**MASTER OF SCIENCE IN APPLIED SCIENCES
(PHYSICAL OCEANOGRAPHY)**

from the

**NAVAL POSTGRADUATE SCHOOL
June 2003**

Author: Michael D. Perry

Approved by: Peter Chu
Thesis Advisor

Eric Gottshall
SPAWAR
Second Reader

Mary Batteen
Chairman, Department of Oceanography

THIS PAGE INTENTIONALLY LEFT BLANK

ABSTRACT

The purpose of this thesis is to determine the effect that the inclusion of satellite altimeter data has on weapon preset accuracy. GDEM data and MODAS data utilizing four satellite altimeters were used by the Weapon Acoustic Preset Program to determine the suggested presets for a Mk 48 torpedo. The acoustic coverage area generated by the program will be used as the metric to compare the two sets of outputs. The assumption is that the MODAS initialized presets will be more accurate, and, therefore, the difference between the two sets of presets can be attributed to inaccuracy on the part of the GDEM presets. Output presets were created for two different scenarios, an Anti-Surface Warfare (ASUW) scenario and an Anti-submarine Warfare (ASW) scenario, and three different depth bands, shallow, mid, and deep. After analyzing the output, it became clear that the GDEM data predicted a weapon effectiveness that was far higher than the effectiveness predicted by the MODAS data. Also, while GDEM predicted a wide range of coverage percentages MODAS predicted a narrow range of coverage percentages.

THIS PAGE INTENTIONALLY LEFT BLANK

TABLE OF CONTENTS

| | | |
|-------------|--|-----------|
| I. | INTRODUCTION..... | 1 |
| A. | BACKGROUND | 1 |
| B. | PURPOSE..... | 1 |
| C. | THESIS SCOPE..... | 2 |
| II. | NAVY’S METOC MODELS AND DATA..... | 3 |
| A. | GENERALIZED DIGITAL ENVIRONMENTAL MODEL | 3 |
| B. | MODULAR OCEAN DATA ASSIMILATION SYSTEM | 5 |
| C. | SATELLITE ALTIMETERS | 7 |
| III. | NAVY’S WEAPON ACOUSTIC PRESET PROGRAM..... | 11 |
| IV. | STATISTICAL ANALYSIS | 15 |
| A. | INPUT AND OUTPUT DIFFERENCE..... | 15 |
| B. | ROOT MEAN SQUARE DIFFERENCE..... | 15 |
| V. | COMPARISON BETWEEN GDEM AND MODAS IN THE GULF STREAM REGION | 17 |
| A. | DATA | 17 |
| B. | OCEAN CONDITIONS | 18 |
| VI | COMPARISON OF WEAPON ACOUSTIC PRESET USING GDEM AND MODAS..... | 25 |
| A. | OUTPUT DISTRIBUTIONS | 25 |
| B. | OUTPUT RMSD | 28 |
| VII | CONCLUSIONS | 33 |
| A. | DISCUSSION | 33 |
| B. | FUTURE WORK..... | 34 |
| | APPENDIX A INPUT HISTOGRAMS | 35 |
| | APPENDIX B INPUT RMSD GRAPHS | 41 |
| | APPENDIX C RMSD PROFILES | 47 |
| | APPENDIX D OUTPUT HISTOGRAMS..... | 65 |
| | LIST OF REFERENCES | 69 |
| | INITIAL DISTRIBUTION LIST | 71 |

THIS PAGE INTENTIONALLY LEFT BLANK

LIST OF FIGURES

| | | |
|------------|---|----|
| Figure 1. | EDE Interface..... | 12 |
| Figure 2. | Acoustic Preset Module Display..... | 13 |
| Figure 3. | Area of Interest | 17 |
| Figure 4. | Detailed Area of Interest | 18 |
| Figure 5. | GDEM Generated Surface Temperature and Salinity Distribution | 19 |
| Figure 6. | MODAS Generated Surface Temperature and Salinity Distribution | 20 |
| Figure 7. | RMSD Profile | 23 |
| Figure 8. | Shallow Depth Band Coverage Percentage Distributions | 26 |
| Figure 9. | Mid Depth Band Coverage Percentage Distributions | 27 |
| Figure 10. | Deep Depth Band Coverage Percentage Distributions | 28 |
| Figure 11. | Acoustic Coverage RMSD for Shallow Depth Band..... | 29 |
| Figure 12. | Acoustic Coverage RMSD for Mid Depth Band | 30 |
| Figure 13. | Acoustic Coverage RMSD for Deep Depth Band | 31 |
| Figure 14. | Temperature Distribution at 0 meters | 35 |
| Figure 15. | Salinity Distribution at 0 meters | 35 |
| Figure 16. | Sound Speed Distribution at 0 meters..... | 36 |
| Figure 17. | Temperature Distribution at 50 meters | 36 |
| Figure 18. | Salinity Distribution at 50 meters | 37 |
| Figure 19. | Sound Speed Distribution at 50 meters..... | 37 |
| Figure 20. | Temperature Distribution at 100 meters | 38 |
| Figure 21. | Salinity Distribution at 100 meters | 38 |
| Figure 22. | Sound Speed Distribution at 100 meters..... | 39 |
| Figure 23. | Temperature Distribution at 2000 meters | 39 |
| Figure 24. | Salinity Distribution at 2000 meters | 40 |
| Figure 25. | Sound Speed Distribution at 2000 meters..... | 40 |
| Figure 26. | RMSD of Temperature at 0 meters..... | 41 |
| Figure 27. | RMSD of Salinity at 0 meters..... | 41 |
| Figure 28. | RMSD of Sound Speed at 0 meters | 42 |
| Figure 29. | RMSD of Temperature at 100 meters..... | 42 |
| Figure 30. | RMSD of Salinity at 100 meters..... | 43 |
| Figure 31. | RMSD of Sound Speed at 100 meters | 43 |
| Figure 32. | RMSD of Temperature at 2000 meters..... | 44 |
| Figure 33. | RMSD of Salinity at 2000 meters..... | 44 |
| Figure 34. | RMSD of Sound Speed at 2000 meters | 45 |
| Figure 35. | RMSD Profile | 47 |
| Figure 36. | RMSD Profile | 47 |
| Figure 37. | RMSD Profile | 48 |
| Figure 38. | RMSD Profile | 48 |
| Figure 39. | RMSD Profile | 49 |
| Figure 40. | RMSD Profile | 49 |
| Figure 41. | RMSD Profile | 50 |

| | | |
|------------|--|----|
| Figure 42. | RMSD Profile | 50 |
| Figure 43. | RMSD Profile | 51 |
| Figure 44. | RMSD Profile | 51 |
| Figure 45. | RMSD Profile | 52 |
| Figure 46. | RMSD Profile | 52 |
| Figure 47. | RMSD Profile | 53 |
| Figure 48. | RMSD Profile | 53 |
| Figure 49. | RMSD Profile | 54 |
| Figure 50. | RMSD Profile | 54 |
| Figure 51. | RMSD Profile | 55 |
| Figure 52. | RMSD Profile | 55 |
| Figure 53. | RMSD Profile | 56 |
| Figure 54. | RMSD Profile | 56 |
| Figure 55. | RMSD Profile | 57 |
| Figure 56. | RMSD Profile | 57 |
| Figure 57. | RMSD Profile | 58 |
| Figure 58. | RMSD Profile | 58 |
| Figure 59. | RMSD Profile | 59 |
| Figure 60. | RMSD Profile | 59 |
| Figure 61. | RMSD Profile | 60 |
| Figure 62. | RMSD Profile | 60 |
| Figure 63. | RMSD Profile | 61 |
| Figure 64. | RMSD Profile | 61 |
| Figure 65. | RMSD Profile | 62 |
| Figure 66. | RMSD Profile | 62 |
| Figure 67. | RMSD Profile | 63 |
| Figure 68. | RMSD Profile | 63 |
| Figure 69. | RMSD Profile | 64 |
| Figure 70. | Shallow Depth ASUW Coverage Percentage Distribution..... | 65 |
| Figure 71. | Shallow Depth ASW Coverage Percentage Distribution..... | 65 |
| Figure 72. | Mid Depth ASUW Coverage Percentage Distribution | 66 |
| Figure 73. | Mid Depth ASW Coverage Percentage Distribution | 66 |
| Figure 74. | Deep Depth ASUW Coverage Percentage Distribution | 67 |
| Figure 75. | Deep Depth ASW Coverage Percentage Distribution | 67 |

ACKNOWLEDGMENTS

To Professor Peter Chu and CDR Eric Gottshall, thank you for introducing me to this topic and giving me the support that I needed to write this thesis. For running the data through the preset program, thank you to David Cwalina and everyone else at NUWC for your help. Also, I would like to thank Dr. Charlie Barron for his effort in preparing the MODAS data. Finally, I would like to thank my wife for all of her loving help and support, and for the long nights that she put in proofing this thesis.

THIS PAGE INTENTIONALLY LEFT BLANK

I. INTRODUCTION

A. BACKGROUND

Even with all the high technology weapons onboard U.S. Navy ships today, the difference between success and failure often comes down to our understanding and knowledge of the environment in which we are operating. Accurately predicting the ocean environment is a critical factor in using our detection systems to find a target and in setting our weapons to prosecute a target. Ocean descriptors such as temperature, salinity, and density profiles are used to model and describe the world's oceans. From these parameters sound velocity profiles (SVP) can be created. SVPs are a key input used by U.S. Navy weapons programs to predict weapon performance in the medium. The trick lies in finding the degree to which the effectiveness of the weapon systems is tied to the accuracy of the ocean predictions.

The U.S. Navy currently relies on three different methods to obtain representative SVPs of the ocean: climatology, in-situ measurements, and data (including satellite data) assimilation. The climatological data provides the background SVP information that might not be current. The Generalized Digital Environmental Model (GDEM) is an example of a climatological system that provides long term mean temperature, salinity, and sound speed profiles. The in-situ measurements such as the conductivity-temperature-depth (CTD) and expendable bathythermographs (XBT) casts may give accurate and timely information, however, they are not likely to have the large spatial and temporal coverage necessary to cover all areas U.S. ships will be operating. The data assimilation system uses climatology as the initial guess and then obtains synoptic SVPs using satellite and in-situ data. The Modular Ocean Data Assimilation System (MODAS) uses sea surface height (SSH) and sea surface temperature (SST) in this way to make nowcasts of the ocean environment.

B. PURPOSE

The current assumption is that MODAS derived SVPs are always better than climatological SVPs. Unfortunately, to the user, the term “better” lacks any tactical significance. How great is the advantage gained from using MODAS field data, and what

is the quantifier used to make the judgment? The question also arises of how many altimeters are necessary to generate an optimal MODAS field. Too few inputs could result in an inaccurate MODAS field, which in turn leads to decreased weapon effectiveness. There must also be some point at which the addition of another altimeter is going to add a negligible increase in effectiveness. This is due to data assimilation saturation, the point at which additional altimeter data can only provide information for a location where data has already been obtained. This superfluous altimeter is then simply a waste of money that could be spent on a useful system. The purpose of this thesis is to quantify the advantage gained from the use of MODAS data rather than climatology. The study will specifically cover the benefits of MODAS data over climatology when using their respective SVP's to determine torpedo settings. These settings result in acoustic coverage percentages that will be used as the metric to compare the two types of data.

C. THESIS SCOPE

While a larger data set with more variety was desired, only the section of ocean between 40° N, 35° N, 75° W, and 70° W was examined, and only the March 15, 2001 MODAS field and climatology data was available. Also, the MODAS data all corresponds to a four altimeter setup. With these limitations in mind, the goals of this thesis were as follows: first, to observe the difference in weapon preset effectiveness between GDEM and MODAS initialized presets, and second, to determine if coverage percentage is an accurate, useful metric in comparing the two groups of presets.

The Weapon Acoustic Preset Program (WAPP) was used to generate the presets and coverage percentage from the corresponding input data. To keep the study simple, but relevant, two tactics were selected to evaluate the weapon settings. The selected tactic types were surface, corresponding to an Anti-Surface Warfare (ASUW) scenario, and submerged, corresponding to a low Doppler Anti-Submarine Warfare (ASW) scenario consistent with diesel operations. For each of the tactics there were three depth bands: a shallow band, a mid band, and a deep band. Each of the depth bands had an effectiveness value associated with it that was a factor of the acoustic coverage within the target depth band.

II. NAVY'S METOC MODELS AND DATA

A. GENERALIZED DIGITAL ENVIRONMENTAL MODEL

The Generalized Digital Environmental Model is a four dimensional (latitude, longitude, depth and time) digital model maintained by the Naval Oceanographic Office. GDEM was generated using over seven million temperature and salinity observations, most of them drawn from the Master Oceanographic Observation Data Set (MOODS). Globally GDEM has a resolution of 1/2° degree. However, in a few select areas, higher resolutions are available (Fox, 2002). In order to represent the mean vertical distribution of temperature and salinity for grid squares, GDEM determines analytical curves to fit to the individual profiles (Teague et. al., 1990)

Before curves are fitted to the data, a quality control protocol is implemented that removes anomalous features or bad observations. The data is checked for proper range and static stability, and it is checked to ensure that it has not been misplaced in location or season. Once the data has been inspected for quality, curves are fitted to the data. From the mathematical expressions that represent the curves, coefficients are determined. It is these coefficients that will be averaged. It can be shown that the coefficients resulting from averaged data are not the same as the averaged coefficients of the data. In order to minimize the number of coefficients necessary to generate smooth curves different families of curves are used for different depth ranges. This necessitates the careful selection of matching conditions in order to ensure that no discontinuities in the vertical gradients occur. Separate computation of temperature and salinity allow the results to be checked against each other to ensure stable densities (Teague et. al., 1990).

The shallow temperature submodel of GDEM covers the part of the water column extending from the surface down to 400m. The squared amplitude response of a Butterworth filter given by

$$R(Z) = \frac{1}{1 + (Z / A)^{2B}} \quad (0.1)$$

is used to model the vertical profile from the surface down to the base of the seasonal thermocline. In this formula, Z is the depth to the thermocline base ($Z = z_1$), A determines the depth of the middle of the thermocline, and B controls the sharpness of the thermocline. The remainder of the water column down to 400 meters ($z_2 = 400$) is fitted with an exponential curve given by

$$E(Z) = x^{ax+b} \quad (0.2)$$

where x is a linear function of Z ($z_1 \leq Z \leq z_2$). When these two formulas are combined with the appropriate offsets and tail yields, the result is a set of two equations describing the fitted temperature as a set of eight coefficients ($T_0, T_{z1}, T_{z2}, z_1, A, B, a, b$). These equations will be fit to any profile that passes quality control and fits within the appropriate timeframe. Should the rms error of the fit be greater than .5° C the profile will be rejected (Teague et. al., 1990).

For temperature and salinities profiles in the depth range 200-2450 m and salinities in the depth range of 0-400 m, a Gram polynomial is used. Their attractive feature is the fact that the computation of high order terms does not require the recomputation of low order terms. Orthogonal polynomials are given by

$$P_{NM}(D) = \sum_{K=0}^M (-1)^K \binom{M}{K} \binom{M+K}{K} \frac{D^K}{N^K} \quad (0.3)$$

for degrees $M = 0, 1, 2, \dots, N$. The functional form is given by

$$\hat{G}(D) = a_0 P_{N0}(D) + a_1 P_{N1}(D) + \dots + a_m P_{NM}(D) \quad (0.4)$$

where D is the depth index and G is either temperature or salinity. M was experimentally determined to be five for the shallow and middle salinity models and seven for the middle temperature model. For both the deep temperature and salinity profiles a simple quadratic polynomial given by

$$F(Z) = c_1 + c_2 Z + c_3 Z^2 \quad (0.5)$$

is used. In this formula, Z is greater than or equal to 2000 m, but less than or equal to the bottom depth (Teague et. al., 1990).

Once all of the coefficients have been determined, a uniform spatial grid of coefficients is created for each profile. The reason behind gridding interpolated coefficients rather than observed values lies in the fact that the average of two profiles will not produce a profile that is representative of either one. On the other hand, averaging the coefficients produces a representative profile that has the appropriate shape and places the thermocline at the average depth (Teague et. al., 1990).

The final step is ensuring that there is vertical continuity between each of the submodels. At the interface between the top and middle submodels, if a temperature difference of 0.25° C or less is observed the difference is added to the top of the middle profile. For differences larger than 0.25° C but smaller than 1.0° C, the difference is split between the top model and the middle model. In the event of difference greater than 1.0° C the difference is split between the top and middle models and then the profiles, not the coefficients, are modified as follows

$$T_{new} = T_z + \alpha \Delta T (0.835)^\beta \quad (0.6)$$

where $\beta = \delta |Z - \text{merge depth}|$, and ΔT is $T_{mid} - T_{top}$ for the top merge and $T_{top} - T_{mid}$ for the middle merge. δ is the scaling factor, 0.01 for the middle model and 0.05 for the top model. The second merge follows a similar process except the merge is at 2000 m. The difference is added to the middle model, and $\delta = 0.02$ (Teague et. al., 1990).

B. MODULAR OCEAN DATA ASSIMILATION SYSTEM

The Modular Ocean Data Assimilation System is a collection of over 100 FORTRAN programs and UNIX scripts that can be combined to generate a number of different products. A few examples of MODAS programs include data sorting, data cross-validation, data assimilation, and profile extension. This modularity allows MODAS to be quickly and easily modified to handle problems or new requirements as they arise. MODAS has varying degrees of resolution starting at 1/2° in the open ocean increasing to 1/4° in coastal seas and increasing again 1/8° near the coast (Fox, 2002). To generate nowcasts and forecasts, the MODAS system uses a relocatable version of the Princeton Ocean Model (POM). To initialize the POM MODAS temperature and salinity

grids, geostrophically estimated currents, or extracted currents from other POM's can be used (Fox, 2003).

One of the most important features of MODAS is its use of dynamic climatology. Dynamic climatology is the incorporation of additional information into the historical climatology in order to portray transient features that are not represented by the climatology. Two useful quantities that are easily gathered from satellites are sea surface height (SSH) and sea surface temperature (SST). While SST from altimeters can be used directly, the SSH, which is measured as the total height relative to the proscribed mean, must be converted into a steric height anomaly in order to be used. Two dimensional (2D) SST and SSH fields are generated from point observations through the use of optimal interpolation.

Optimal interpolation is a process by which the interpolated temperature or salinity anomaly is determined as the linear combination of the observed anomalies. Each of the anomalies is given a weight which accounts for variation in temporal and spatial sampling. Weights are computed by minimizing the least square difference between the interpolated value and the true value at the grid point and by solving the equations

$$\sum_{j=1}^N \alpha_j \mu_{ij} + \lambda^{-2} \alpha_i = \mu_{Gi} \quad (0.7)$$

where α_i are the weights, λ is the signal to noise ratio, μ_{ij} is the autocorrelation between locations i and j, and μ_{Gi} is the autocorrelation between the grid point and i. For each grid node location matrix inversion is used to solve the system of N equations for the N unknown weights. The other parameters are computed using the first guess field, MOODS profiles, and climatology. Using this process any new observation can be interpolated into the appropriate MODAS grid node.

The first guess field, the prior days 2D SST field, or the weighted average of 35 days of altimeter data respectively, is subtracted from the new observations, and the resulting deviations are interpolated to produce a field of deviation. This is added to the first guess field to generate the new 2D field. For the first iteration of the optimal interpolation, climatology is used for SST and the SSH measurement is assumed to have

a zero deviation. This means that until the field deviates from the climatology, the extra data has added no value and MODAS reverts to climatology (Fox, 2002).

Once the data is in a useful form, MODAS begins with the climatology profile and then correlates variations in the SSH and SST to variations in the subsurface temperature. The regression relationships used here were constructed by performing a least-squares regression analysis on archived temperature and salinity profiles. This is a three step process starting with the computation of regional empirical orthogonal functions from the historical temperature and salinity profiles. The second step is to express the profiles in terms of an empirical orthogonal function series expansion. The final step is to perform regression analysis on the profile amplitudes for each mode, truncating the series after three terms. This is possible because of the compactness of the empirical orthogonal function representation (Fox, 2002).

Once the subsurface temperatures have been revised, MODAS adjusts the subsurface salinity profile using the relationship between temperature and salinity. This new profile is referred to as a synthetic profile. Synthetic profiles only use these regression relationships down to a depth of 1500 m due to the decreasing reliability of the relationships at depth (Fox, 2002).

MODAS is also able to include measurements from in-situ CTDs and XBTS. The first guess field is the field generated by the dynamic climatology, and the in-situ profiles are subtracted from it to get residuals. Optimal interpolation is once again used to update the temperature field and from the temperature field the salinity field can be generated. This salinity field then serves as a first guess field for the inclusion of the salinity profiles (Fox, 2002).

C. SATELLITE ALTIMETERS

The Navy currently uses satellite altimeters to measure SSH that affect their operations. Of primary interest is mesoscale variability. Meandering fronts and eddies can significantly change the temperature and salinity structure of the ocean. This importance is clearly seen in sonar dependent operations such as ASW. Sonar range can be greatly helped or hindered by the acoustic environment created by the salinity,

temperature, and density. Altimeters also provide the SSH and SST measurements that MODAS uses in its optimal interpolation.

While monitoring mesoscale variability is of prime importance to the Navy, an emerging secondary role for Navy altimeters is monitoring continental shelf and coastal zones. As the Navy conducts more and more operations in littoral waters, the ability to predict near-shore parameters will have increasing importance. Altimeter data can be used to get up-to-date information on rapidly changing near-shore characteristics such as tides and wave height. These are important issues for anyone dealing with mine detection, beach operations, or ship routing.

Altimeters have also been used to measure the flow through important straits, such as the Tsushima Strait, and to measure large-scale circulation. The first of these helps researchers and modelers to develop constraints on local numerical models. Large-scale circulation measurements can also help in the development of models by aiding in error correction. They also help explain the local environment which is often affected by not just local forcing, but large-scale circulation variations as well.

Satellite altimeters can provide a great variety of data, but no single altimeter can provide measurements on all desired time and length scales. Different parameters must be sampled at different frequencies if they are going to be of any use. For instance, sea surface height must be sampled every 48 hours while wave height must be sampled every three hours. While different ocean features all have different time and spatial scales, only the requirements for observation of mesoscale features are presented here as an example (Jacobs et. al., 1999).

In order for an altimeter to efficiently and accurately sample mesoscale features, there are several requirements placed on its accuracy, orbit, and repeat period. A satellite altimeter must produce measurements that are accurate to within 5 cm, or the errors that propagate down into the temperature and salinity calculations will be unacceptable. With an error of only 5 cm, the error in the temperature calculation can be 1-2° C . Satellites should also have an exact repeat orbit to maximize the usefulness of the data collected. Without an exact repeat orbit the only way to get differences in sea surface heights is to use only the data from points where the satellite crosses the track of another altimeter or

itself. An exact orbit is considered to be a 1 km wide swath of a predefined ground track. Finally, the period of a single satellite should be greater than the typical 20 day time scale of a mesoscale feature. If two satellites are used, then they should be spaced so that a point on the ground is not sampled more than once in a 20 day period (Jacobs et. al., 1999).

As described earlier, systems such as MODAS rely heavily on the information provided by these satellites. MODAS uses interpolation to estimate SSH at points that the satellite did not cover. If the ground track spacing is too coarse, then the optimal interpolation scheme of MODAS will begin introducing errors into the fields between the tracks. It is important that the satellites be properly set up so that a maximum amount of information can be gathered with a minimum amount of error (Jacobs et. al., 1999).

THIS PAGE INTENTIONALLY LEFT BLANK

III. NAVY’S WEAPON ACOUSTIC PRESET PROGRAM

The Weapon Acoustic Preset Program (WAPP) is an automated, interactive means of generating Mk 48 and Mk 48 ADCAP acoustic presets and visualizing torpedo performance. It combines the Mk 48 Acoustic Preset Program (M48APP) and the Mk 48 ADCAP Acoustic Preset Program (MAAPP) into a single integrated package. The M48APP is also employed by the Royal Australian Navy as a part of the Collins Class Augmentation System (CCAS). The Royal Canadian Navy has rearchitected the M48APP for Java. The program is based around a graphical user interface that allows the user to enter the environmental, tactical, target, and weapon data. With these user specified parameters, the program then performs a series of computations to generate accurate acoustic performance predictions. The output includes a ranked listset of search depth/pitch angle/LD/effectiveness values, an acoustic ray trace, and a signal excess map (NUWC, 2002).

The Environmental Data Entry Module (EDE), shown in Figure 1, is a simple Graphical User Interface (GUI) that allows the user to enter a variety of environmental parameters. The sea surface fields allow the user to specify wind speed, wave height, and sea state based on either the World Meteorological or Beaufort scale conventions. The three fields are coupled so that an entry into one field will bring up the appropriate default values for the others. The bottom condition field allows the user to specify the bottom depth and to choose the bottom type from a list of possibilities. The bottom of the GUI is devoted to the water column characteristics and a sound speed profile. The temperature, sound speed, and depth are all in the appropriate English units. The volume scattering strength (VSS) is in dB. The additional fields include the latitude, longitude, the profile name, and the table group identifiers (NUWC, 2002).

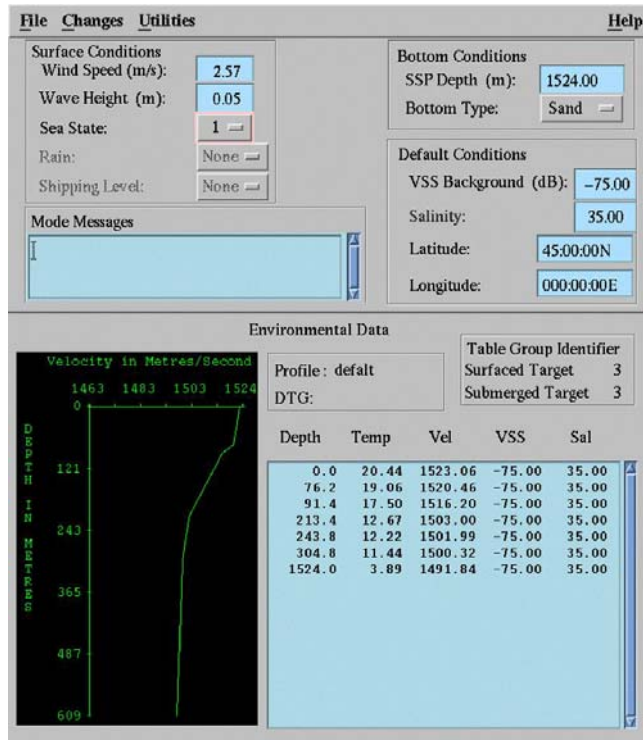


Figure 1. EDE Interface

Once the environmental parameters have been entered, then the user can move on to the Acoustic Module Preset Display, shown in Figure 2. This GUI allows the user to specify a number of parameters about the weapon, the target, and the way the weapon should search. The listset on the right side of the GUI displays a series of search depths, pitch angles, laminar distances, and effectiveness values. The effectiveness values for the various presets are based on expected signal excess and ray trace computations. Both plots can viewed from a pull-down menu. These provide a visual representation of the acoustic performance of the Mk 48 (NUWC, 2002).

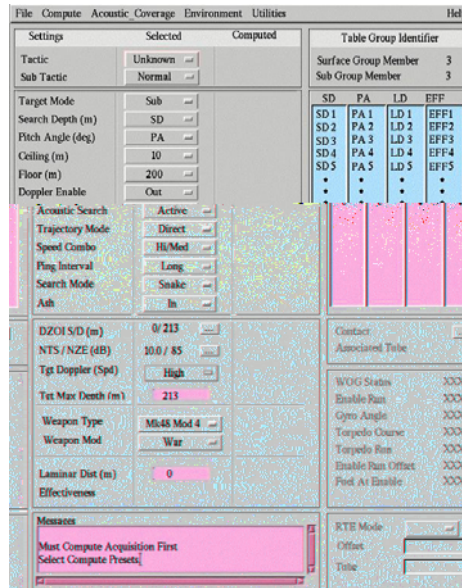


Figure 2. Acoustic Preset Module Display

In addition to automatically computing the most effective preset combination for a given set of environmental parameters, the program also allows the user to manually examine the effectiveness of any allowable preset combination via the signal excess and ray trace plots. The program also allows the user to save the tactical preset list and the accompanying environmental data. The data is stored locally to the weapon module and can be recalled later or transferred via a network to the combat control system (NUWC, 2002).

THIS PAGE INTENTIONALLY LEFT BLANK

IV. STATISTICAL ANALYSIS

A. INPUT AND OUTPUT DIFFERENCE

The difference of the two sets of input METOC data (GDEM and MODAS) ψ_{input} or the two sets of output weapon preset data (running using GDEM and MODAS) ψ_{output}

$$\Delta\psi(\mathbf{r},t) = \psi_M(\mathbf{r},t) - \psi_G(\mathbf{r},t) \quad (0.8)$$

represents the ocean data update using satellite and in-situ observations (input) and the effect of using satellite and in-situ observations on the weapon preset (output). Here ψ_M and ψ_G are the variables (either input or output) using GDEM and MODAS, respectively. We may take the probability histograms of ψ_M and ψ_G to show the difference of the statistical characteristics.

B. ROOT MEAN SQUARE DIFFERENCE

GDEM and MODAS have different grid spacing: $1/2^\circ \times 1/2^\circ$ in GDEM and $1/12^\circ \times 1/12^\circ$ in MODAS. For a GDEM cell, one data is available for GDEM and 36 data for MODAS. The root-mean-square difference (RMSD),

$$\text{RMSD} = \sqrt{\left[\frac{1}{N} \sum_{i=1}^N (\psi_M^{(i)} - \psi_G)^2 \right]} \quad (0.9)$$

is commonly used to represent the difference in the input and output data. Here, N ($=36$) is the total MODAS data number in a GDEM cell. The RMSD can be computed for either the input data to the weapon preset model such as the temperature, salinity, or sound speed, or it can be computed for the output data such as nondimensional detection area. The RMSD computed from the input values are all in International units, but have not been normalized due to the incredibly small values that would result. While it would have been possible to normalize these values and then scale them up, the simplest solution was to use the unnormalized values. The RMSDs from the output data are

unitless because the output values from the preset program are normalized. In addition to the RMSD, basic statistics such as the mean

$$\bar{X} = \frac{1}{N} \left(\sum_{i=1}^N X_i \right) \quad (0.10)$$

and the standard deviation

$$s = \sqrt{\left(\frac{1}{N-1} \left(\sum_{i=1}^N (X_i - \bar{X})^2 \right) \right)} \quad (0.11)$$

have been used.

The assumption is that the MODAS field will be more accurate. What needs to be determined is how differences in MODAS and GDEM data propagate down to the weapon presets.

V. COMPARISON BETWEEN GDEM AND MODAS IN THE GULF STREAM REGION

A. DATA

In order to make a meaningful comparison of MODAS and GDEM data, a sufficiently large data set had to be obtained. The Area of Interest (AOI) also needed to be an area where the ocean environment fluctuated on a fairly short time scale. The GDEM and MODAS data from March 15, 2001 was obtained for the area off the North American coast corresponding to 40° - 35° N latitude and 75° - 70° W longitude. An overview of the area is shown in Figure 3. Figure 4 shows the location of the GDEM and MODAS profiles.

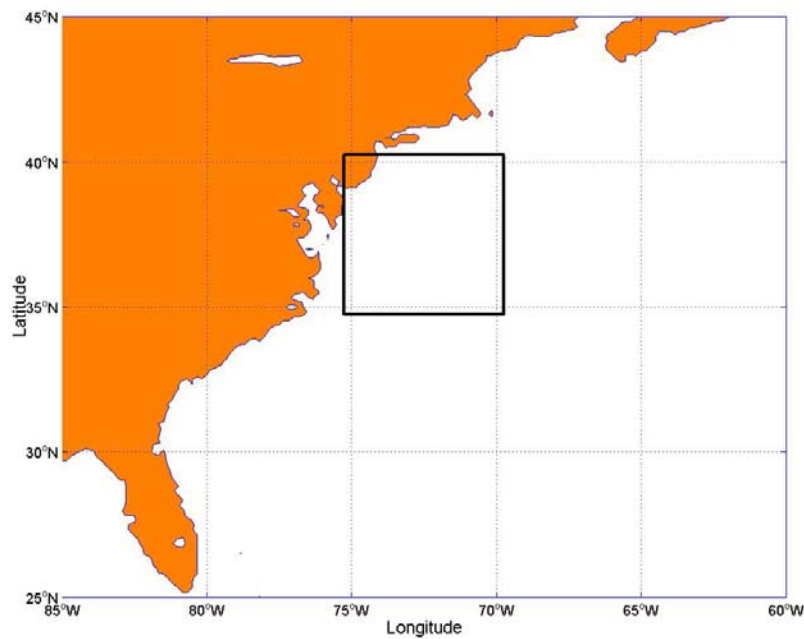


Figure 3. Area of Interest

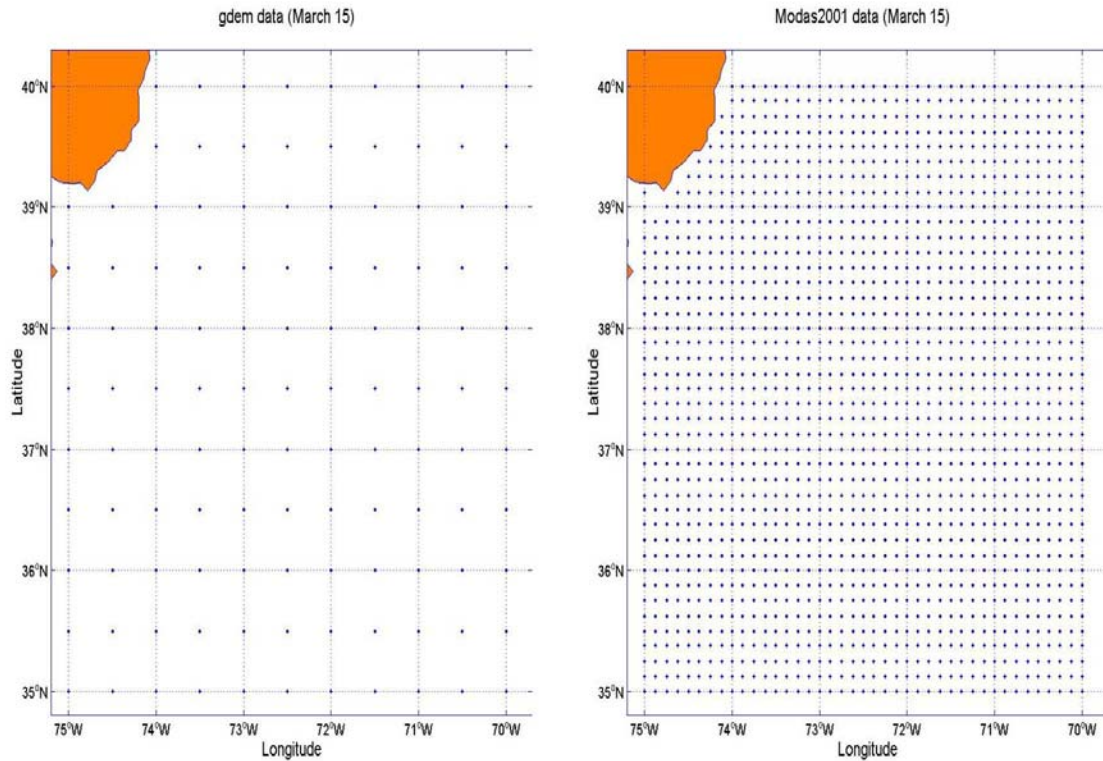


Figure 4. Detailed Area of Interest

Due to the differing resolutions of GDEM and MODAS, this area provided 117 GDEM profiles and 1633 MODAS profiles. Each profile was simply a text file that consisted of a header row and columns of data. The header row contained the number of depths the profile covered, the file's name and the latitude and longitude of the profile. The columns corresponded to depth in feet, the temperature in degrees Fahrenheit, the sound speed velocity in feet per second, a volume backscatter value, and salinity in practical salinity units (psu). Despite the common use of International units in scientific experiments, it was necessary for the profiles to be set up in the appropriate English units. The Weapon Acoustic Preset Program (WAPP), the program used to generate the presets from the profiles, requires inputs to be in English units.

B. OCEAN CONDITIONS

While GDEM and MODAS will often give overall similar pictures of the ocean environment at a given place, MODAS is known to provide more accurate interpretations of the environment. The amount of accuracy MODAS adds is in proportion to the scale

on which ocean parameters vary. For areas such as the Gulf stream, where environmental factors are known to vary rapidly on a relatively small time scale, it is expected that there would be at least a few areas where the two data sets differ. It is these areas that are of particular interest since the difference in the weapon presets should be greatest.

On the surface, the GDEM data provided a view of the temperature distribution that consisted of smooth, uniformly spaced lines of constant temperature that were consistent with the overall flow of the region (Figure 5). The cool water on the shelf gradually gives way to the warm water flowing north along the Gulf stream. The GDEM generated surface salinity distribution is similar to the surface temperature distribution and is consistent with the Gulf stream region. Fresher water lies inland and the salinity increases with distance from the shore. The only variation is in the northeastern section where there is a slight intrusion of the salty offshore water.

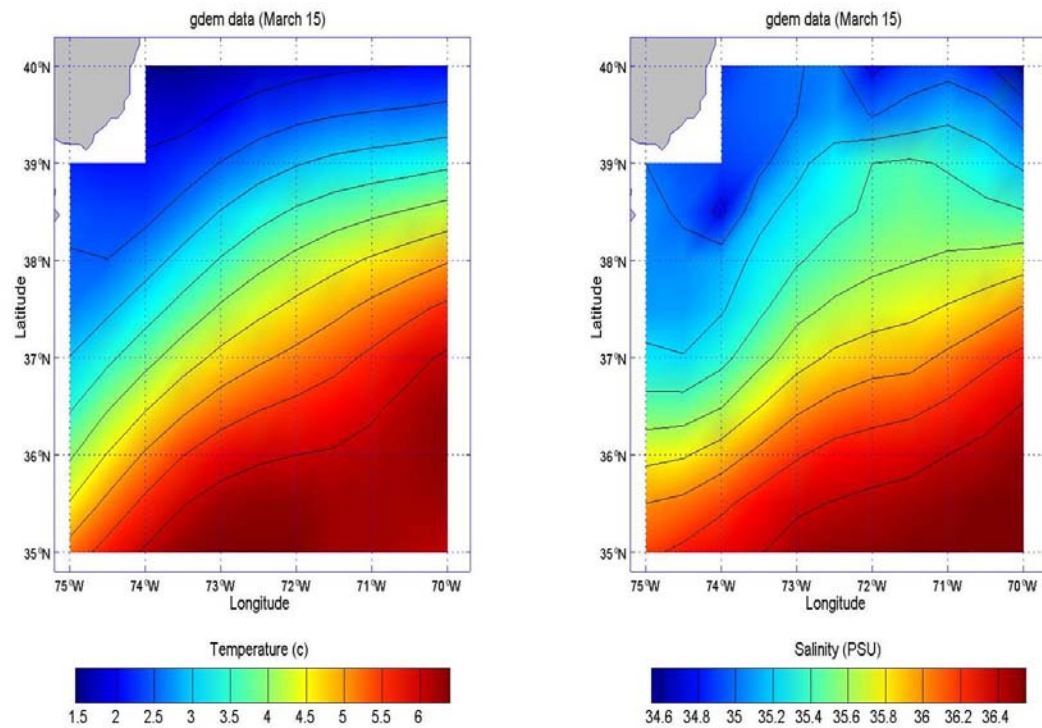


Figure 5. GDEM Generated Surface Temperature and Salinity Distribution

Overall, the GDEM and MODAS distributions are, overall, fairly similar in both their range of values and overall distribution. They are similar to each other in shape, and both show areas of cool fresh water near the coast and areas of warm salty water lying offshore. There are, however, a few differences, with the intrusion of warm salty water in the northeastern section of the MODAS figure (Figure 6) being the most notable. There is also an area of high temperature in the lower right corner of the MODAS figure that does not show up in the GDEM figure. In general the MODAS figure shows the water increasing in temperature and salinity much more rapidly as the distance from the coast increases. The GDEM figure shows a gradual increase in temperature and salinity starting in the top left corner and continuing almost entirely down to the lower right corner. The MODAS figure shows the water reaching maximum temperature and salinity quickly and then staying constant to the lower right corner.

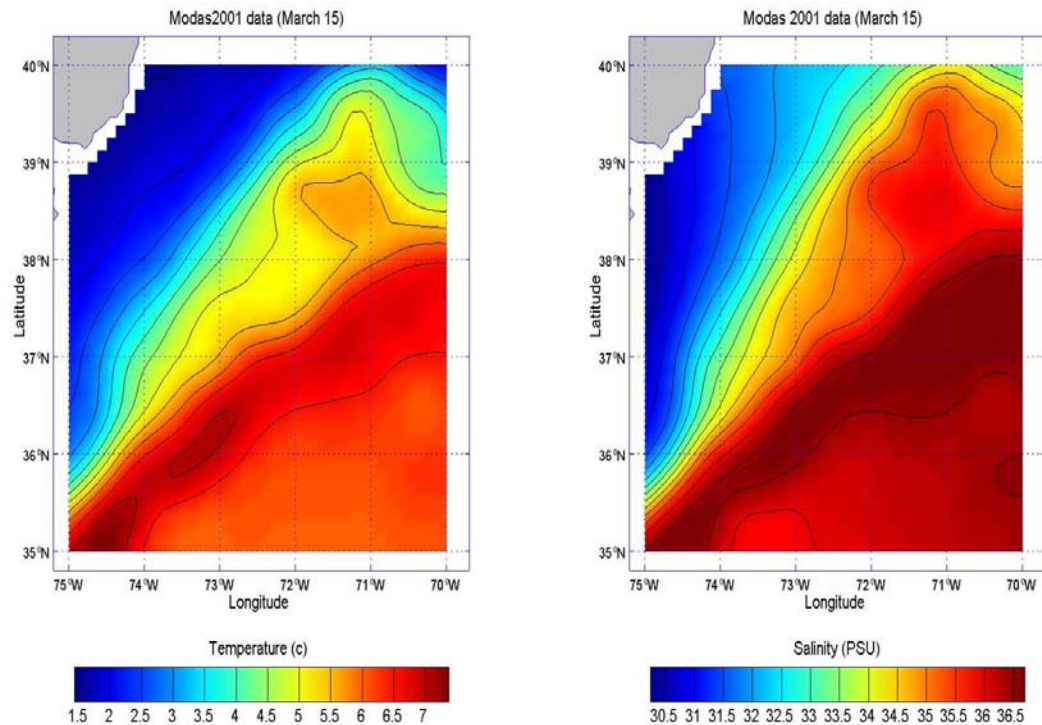


Figure 6. MODAS Generated Surface Temperature and Salinity Distribution

While the GDEM and MODAS data offer similar ranges of temperatures, salinities, and sound speeds at the surface, the distribution of the values is quite different. The histograms in Appendix A reveal that while the temperature values reported by both data sets are similar, the MODAS data has a higher proportion of profiles located in the 6°-7° C range. The difference in the salinity graphs is even more drastic with the bulk of the GDEM values located in the middle of the range and the MODAS values split between the high and low ends of the range. The sound speed graph indicates that MODAS typically reported higher sound speeds than did the GDEM data. This is not too surprising since sound speed in the upper water column tends to be tied closely to temperature, and the MODAS data indicated warmer water than the GDEM data.

Increasing depth to 50 m and then 100 m, it is clear to see that, for temperature, the distribution of the values over the range for both sets of data is quite similar. There is still a slight preference in the MODAS graphs towards higher temperatures, but it is not as drastic as was seen on the surface. Salinity is much the same, with the difference in shapes of the two figures more a factor of the small number of GDEM profiles as compared with the number of MODAS profiles. Sound speed is the only area where the two data sets continue to diverge. From the 50 m and 100 m depth sound speed figures, it is clear that, with depth, the MODAS data indicates increasing sound speed and the GDEM data predicts some sort of sound speed minimum at depth. This is causing the peak on the MODAS graph and the peak on the GDEM graph to move away from each other as depth increases.

By 2000 m the temperature and salinity histograms for the two data sets are virtually identical. At this point any perceived difference in the two is solely a factor of the difference in the number of profiles between the two data sets. For the sound speed figures, this is the point of maximum separation. The GDEM data indicates low sound speeds representative of a deep sound channel, whereas the MODAS data indicates that the sound speed has increased to this point. This lack of a deep sound channel in the MODAS data is of great importance and is difficult to explain given the similarity between the MODAS and GDEM temperature and salinity data at this depth. After this point the GDEM values begin rising again to match the MODAS data.

While the distribution of the values over the range is a useful tool in examining the inputs, it is the difference between the inputs that is of real importance. The figures in Appendix B show the RMSD of the inputs for a variety of depths. From the surface temperature figure in Appendix B, the RMSD of temperature peaks out in the lower left corner of the area of interest (AOI) at about 2° C. Besides the peak, the other significant area is the ridge starting in the lower left corner and running to the middle top of the figure. This corresponds to a narrow region where the GDEM distribution warmed slower than the MODAS distribution moving from the coast out to sea. The warm water intrusion is represented by the gradual increase in height of the ridge. The salinity difference at the surface is nearly zero for most of the AOI and reaches its maximum value of 4.5 PSU along the top of the region. The derived sound speed RMSD, as expected, is smallest far from the coast where the difference in temperature and salinity is smallest and increases towards the coast.

As depth increases, the RMSD in temperature and sound speed changes slowly, but the difference in salinity drops off quickly. Neither the temperature nor sound speed difference changed significantly, but by 100 m depth the RMSD for salinity has gone down to values of less than .8 PSU. Below 100 m depth, the temperature difference begins to decrease slowly. By 2000 m depth the RMSD for both temperature and salinity has dropped to negligible levels for most of the AOI. This is expected since MODAS reverts to climatology at depth.

Except for the profiles in the northwestern corner of the AOI that did not run as deep as the other profiles farther from the coast, all the RMSD vs. depth profiles were remarkably similar. All of the temperature differences showed either a gradual decrease in the difference down to about 1000 m depth or a slight increase in the difference immediately followed by a gradual decrease in the difference down to 1000 m depth. At about 1000 m depth the temperature differences all rapidly dropped to near zero. The sound speed profiles all show the difference increasing down to a maximum value of 60 m/s at around 2000 m depth. After that the RMSD drops off, and by 3000 m depth it has approached zero. The cause of the maximum at 2000 m depth is the lack of a deep sound channel according to the MODAS data. The MODAS profiles almost all have the sound speed steadily increasing down to the maximum depth whereas climatology indicates a

sound speed minimum at 2000m. While there is some variation in how quickly the salinity differences drop to near zero, they are less than 1 PSU by 200 meters. A few of the profiles do show a minor salinity RMSD spike after 2000 meters, however the magnitude of the spike is never more than .02 PSU and can be attributed to the difference in the resolutions of GDEM and MODAS. Shown in Figure 7 is a representative RMSD profile. The features mentioned above are all clearly visible in this profile. This profile corresponds to the $1/2^\circ$ by $1/2^\circ$ box around the point 37.5° N 71.0° W. For further examples, reference Appendix D.

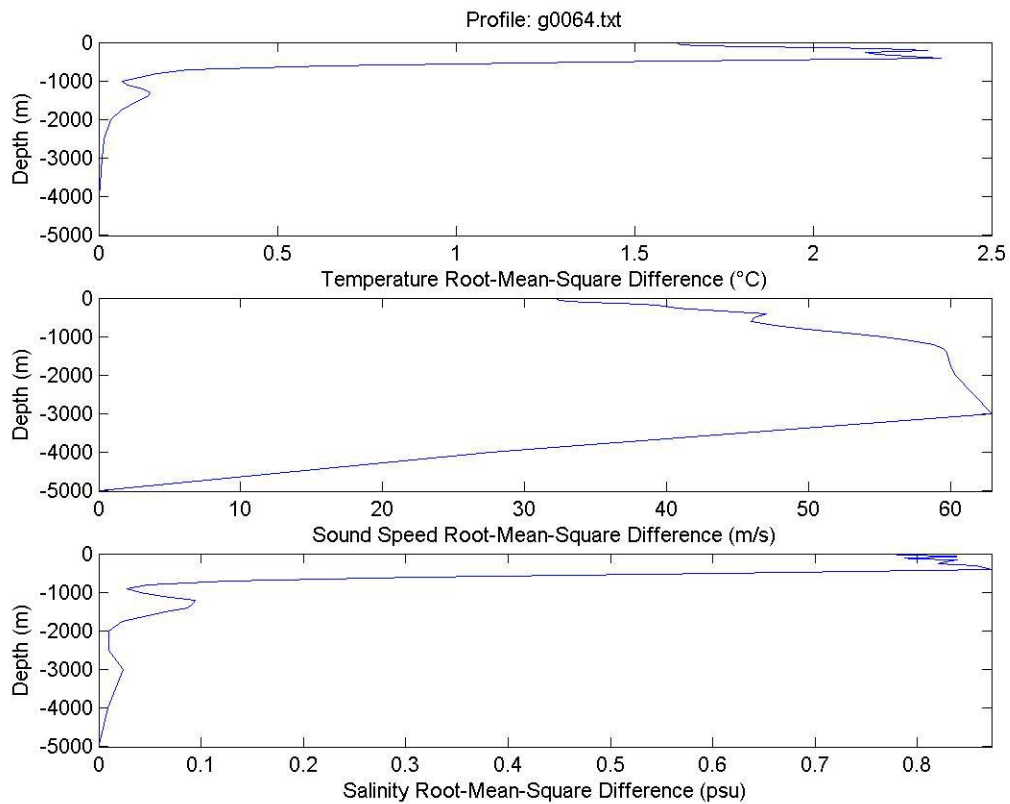


Figure 7. RMSD Profile

THIS PAGE INTENTIONALLY LEFT BLANK

VI COMPARISON OF WEAPON ACOUSTIC PRESET USING GDEM AND MODAS

The raw data was processed by the Naval Underwater Warfare Center (NUWC) Division Newport. They received the input profiles, ran them through the WAPP, and generated the output. Percentage coverage was calculated based on both surface (ASUW) and submarine (ASW) scenarios. The submarine scenario is a low Doppler scenario consistent with diesel submarine operations. The coverage percentages represent coverage in the target depth band, either shallow, mid, or deep. The coverage percentages were also normalized over acoustic modes to produce an output that was unitless.

A. OUTPUT DISTRIBUTIONS

The output provided by NUWC from the WAPP runs consisted of twelve different percentage coverage groups, three depth bands times two scenarios times the two different types of input data. For the non-SVP derived WAPP inputs, consistent values were used throughout the runs to ensure that any difference in the outputs was a result of differences in the GDEM and MODAS data. For each of the groups, basic statistics such as mean, maximum, minimum, and standard deviation were computed and then the data was constructed into histograms (Appendix D) to give a visual representation of how the data was distributed.

In the shallow depth band ASUW scenario both MODAS and GDEM yielded mean coverage percentages that were very close to each other (Figure 8). While statistically speaking the means are different, in real world applications a few percentage points difference is negligible. From a users standpoint this means that both sets of data predicted about the same mean coverage for the AOI. The ASW scenario yielded similar results except for the fact that the two means were not even statistically different. While this seems to indicate that the two data sets are returning similar results, there are some important differences. First are the outliers on the GDEM graphs. Values in the high thirties to low fifties are extremely rare, yet the GDEM data indicate that in at least one location for the ASUW scenario and several for the ASW scenario, the weapon will perform to this level. The ASW scenario also had a rather significant number of GDEM

profiles that generated below average coverage percentages. This would indicate that GDEM predicts that coverage will vary greatly with location. In comparison the MODAS values for both scenarios tended to be very consistent. Coverage percentage varies little with location due to the fact that most of the profiles lie within a very narrow range. Overall GDEM predicts excellent coverage some of the time and poor coverage the rest of the time. MODAS data on the other hand, indicates that coverage percentage will not be excellent anywhere but the expected values will be uniform over the whole shallow depth band region.

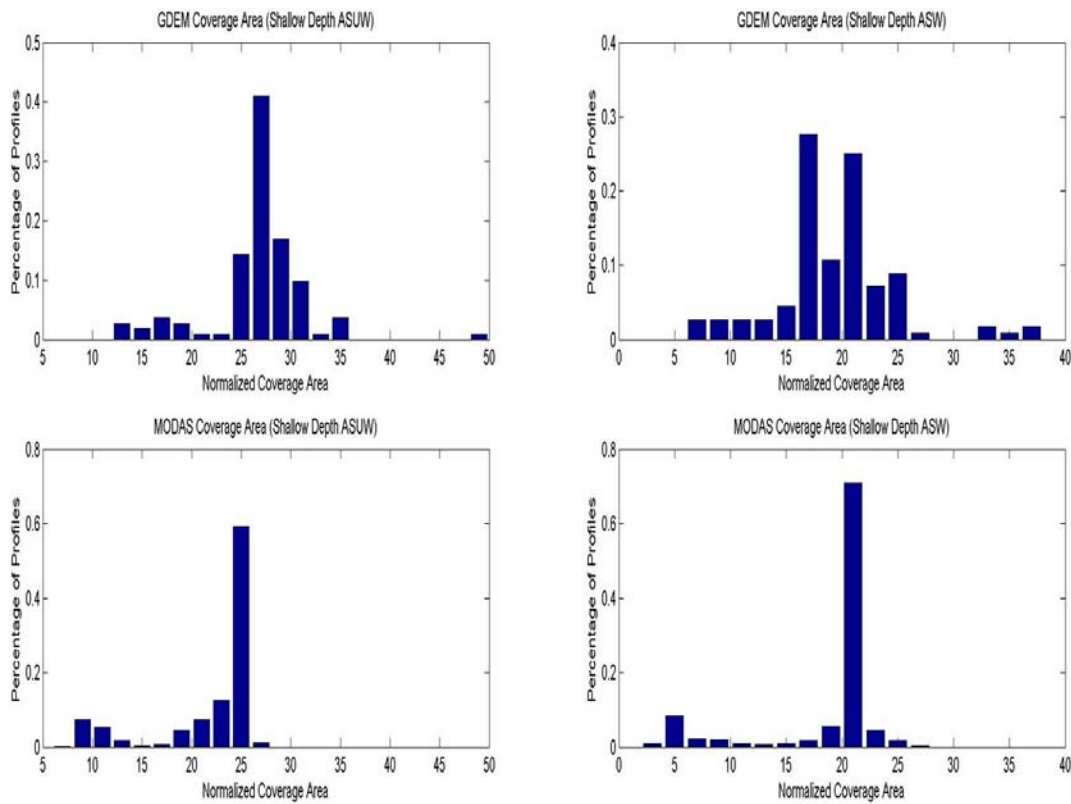


Figure 8. Shallow Depth Band Coverage Percentage Distributions

The mid depth band yielded results (Figure 9) that were similar in distribution to the shallow depth band. Across both scenerios the mean coverage of the GDEM data and the mean coverage of the MODAS data were statistically identical. Outliers were once again observed in the GDEM data, the larger outlier in the ASUW scenario, and the greater number of outliers in the ASW scenario. The wide dispersion of the GDEM

derived coverages indicates that weapon effectiveness will vary depending on location. This is similar to the predictions for the shallow depth band and would indicate that GDEM predicts a water column that has varying coverage values depending on horizontal and vertical location. MODAS data once again indicates an overall performance in the region that is slightly less than the GDEM prediction; however, the MODAS data is grouped even more tightly than in the shallow depth band. The coverage in the ASW scenario in particular varies little about the mean value. This and the shallow depth band predictions indicate uniform coverage can be expected even at some depth.

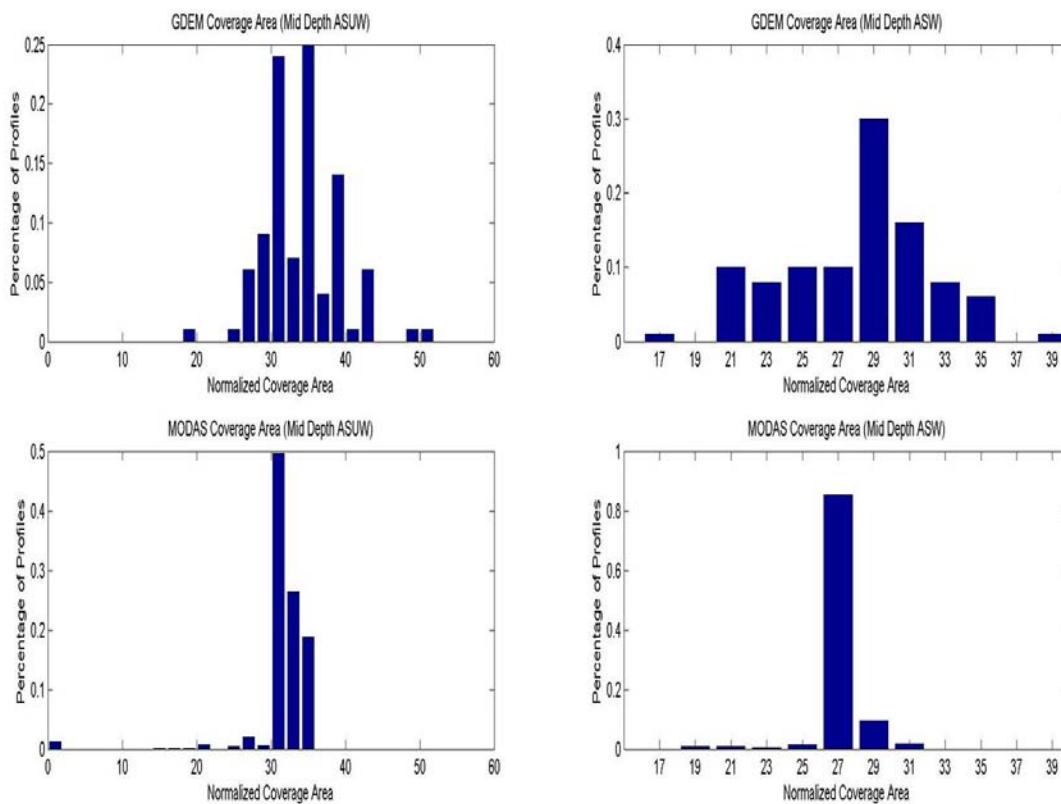


Figure 9. Mid Depth Band Coverage Percentage Distributions

In the deep depth band the graphs take on a slightly different shape (Figure 10), but they convey much the same meaning. In both scenarios the GDEM graphs are weighted heavily to the right end, predicting that in the deep depth band coverage will be very good over most of the area. The ASUW scenario has the larger predicted values, but the values in the ASW scenario are still on the upper end of what is normal. The MODAS

data predicts performance that is, while not particularly bad, still much more pessimistic than the GDEM predictions. For both scenarios the means of the GDEM and MODAS derived predictions are statistically different with the MODAS data providing the smaller mean in both scenarios. Although the dispersion of the GDEM data is large in both scenarios, the data is so heavily weighted towards the upper end that low GDEM coverage percentages are average values for the MODAS data coverage percentages. The MODAS data coverage percentages are once again tightly grouped; the uniformity of the predicted coverage percentages observed in the two other depth bands extends from the surface down to the selected maximum operating depth.

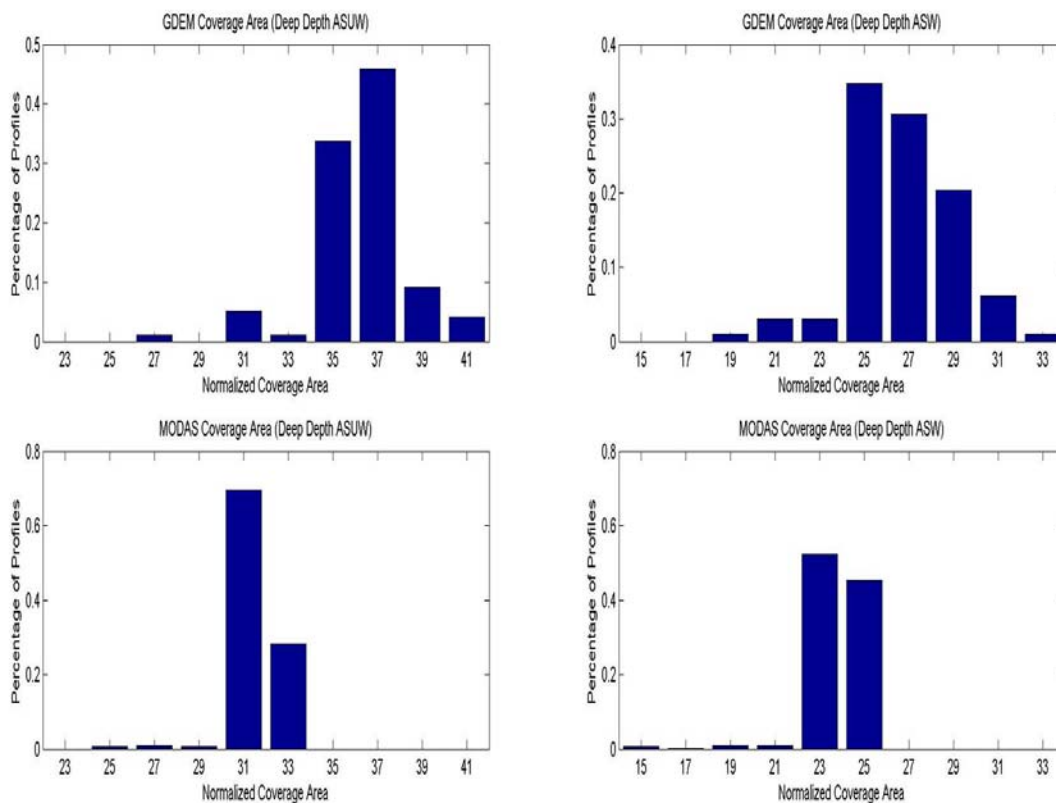


Figure 10. Deep Depth Band Coverage Percentage Distributions

B. OUTPUT RMSD

For the shallow depth band, the RMSD in the percentage coverage area (Figure 11) was small over most of the AOI, consistent with the similar means and range of

values noted in the previous section. The areas computed to have small RMSD coverage percentages also had small RMSD in temperature and salinity. In the region where the RMSD in temperature and salinity was largest, though, a large RMSD in percentage coverage is also observed. These larger values are likely areas where the GDEM data generated overly optimistic coverage percentage predictions. For the surface scenario, RMSDs of up to 25 percent are shown in the region around 39° N 73° W, and the warm salty intrusion observed on the MODAS data coincides with a second peak in the northeastern section of the graph. Overall the ASW scenario shows RMSDs that are similar to the ASUW scenario, the only difference being that the values are, on average, slightly smaller. The notable exception is the peak located at the top portion of the graph.

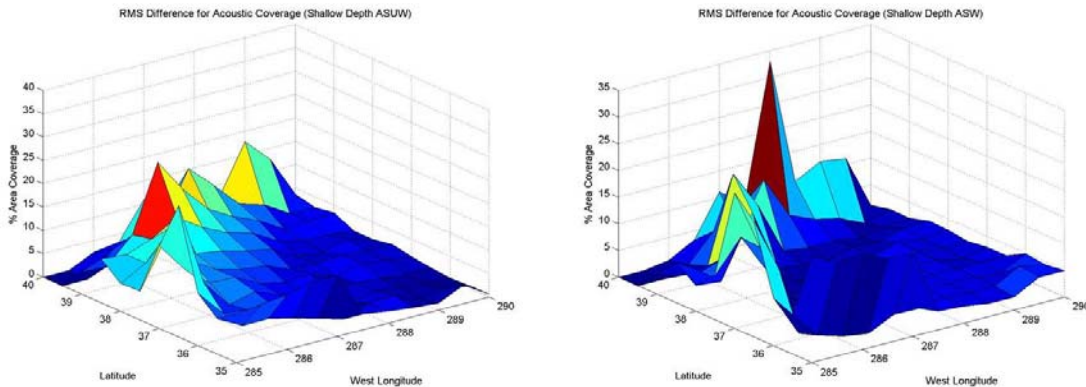


Figure 11. Acoustic Coverage RMSD for Shallow Depth Band

Figure 12 shows the mid depth band RMSD. For the mid depth band the percentage coverage RMSD for the ASUW scenario is simply a scaled down version of the shallow depth band ASUW graph. This is due to the coverage percentage distributions for the shallow and mid depth ASUW scenarios being very similar. The major difference is in the ASW scenario. The single exceptional peak at the top of the previous graph is gone and the observed differences have become much smaller. Most of the RMSD for the mid depth ASW scenario do not exceed 10%. This is probably due to nearly identical coverage percentage means from both data sets, and the tighter grouping of the GDEM data coverage percentage predictions in the mid depth band ASW scenario.

The RMSD values are small even in the areas where the temperature and salinity differences were observed to be large, such as in the upper section of the graph

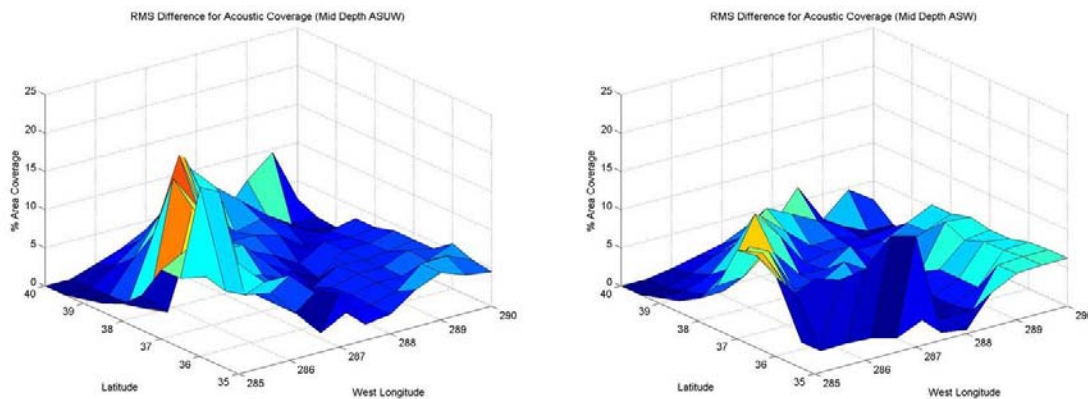


Figure 12. Acoustic Coverage RMSD for Mid Depth Band

The RMSDs observed in the deep depth band scenarios (Figure 13) were smaller than those of the shallow depth band, but similar in magnitude to the mid depth band. For the ASUW scenario the RMSD peaks near the northwestern corner of the AOI and then decreases steadily in steps heading toward the opposite corner. While the individual RMSD values seen are not as large as some of the ones in the other depth bands, more of the area has a non-negligible RMSD. The cause of this can be seen from the percentage coverage distribution for the deep depth ASUW scenario. The GDEM data resulted in values that were almost all larger than the largest MODAS derived values. This overly optimistic prediction means that over a large portion of the AOI, the RMSD is going to be non-zero. The RMSD in the ASW scenario changes very little from the mid depth band save for the fact that the values in the lower right corner are smaller. The coverage distributions for the deep ASW scenario were similar to the ASUW case, but the separation between the two means was not so pronounced. The result is a larger region where the RMSD is small or zero.

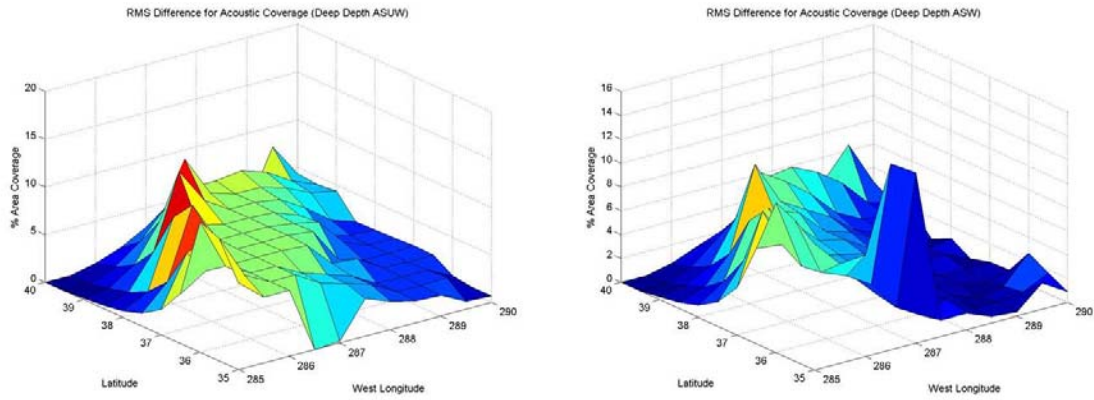


Figure 13. Acoustic Coverage RMSD for Deep Depth Band

Both of these graphs match the pattern that has so far been observed in the other depth bands. The ASUW scenario has the higher RMSD values, with areas of both high temperature and salinity differences corresponding to peaks on the graphs. The RMSD values also approach zero moving toward the top left or bottom right corners. Also, as depth increases, the difference between the two data sets decreases causing the difference between the coverage percentages to decrease.

THIS PAGE INTENTIONALLY LEFT BLANK

VII CONCLUSIONS

A. DISCUSSION

By looking at the RMSD in the temperature and salinity fields generated from the GDEM and MODAS data, it is possible to look for areas where the data differ significantly. It is at these points that the difference in the preset effectiveness should be the greatest. This was observed for both scenarios at all depth bands. The percentage coverage was the most different at points where both the temperature and salinity RMSD was large. This was particularly true for the shallow depth band where differences of 25% were observed for both scenarios. It is of interest to note that even at the surface the RMSDs for the temperature and salinity were never more than a few degrees or psu. Even with only this slight increase in the accuracy of the inputs, a large increase in the correctness of the predicted weapon effectiveness occurred. This seems to imply that the sensitivity of the presets to changes in the inputs is quite high.

From the output distributions it appears that the GDEM derived coverage percentages indicate that a wide range of weapon effectiveness will be observed in the AOI. In some areas coverage will be very high and in others the coverage will be very poor, but the overall tendency is for the coverage to be high for any given area. This tendency towards high predicted weapon effectiveness can be attributed to the GDEM data's indication of a deep sound channel. The MODAS derived percentages seem to reveal that the exact opposite is true. A narrow range of coverage percentages will be observed, with the average predicted coverage being lower than the average predicted coverage for GDEM. As noted earlier, the lack of a deep sound channel in the MODAS data caused the predicted coverage to be lower than the corresponding GDEM coverage predictions. The narrower range of coverage values observed in the MODAS runs is consistent with the fact that the MODAS data indicated a water column that happened to be significantly more uniform than the straight climatology would have predicted.

The difference in the resolution between MODAS and GDEM must also be taken into account. At locations where the GDEM and MODAS data overlap the predicted acoustic coverage percentages tend to be reasonably close though not identical. Between

these locations the higher resolution of the MODAS data allows for a more gradual change in the coverage. The lower resolution of the GDEM data makes it seem as though the change in coverage occurs very rapidly over a short distance. Since for every GDEM point there were sixteen MODAS points areas where changes were gradual appear as large RMSDs in the graphs. This can make it seem that the difference in predicted coverage between MODAS and GDEM for a given area is larger than it really is..

Still, these are important results since prediction of weapon effectiveness is vital to mission planning and execution. In this case an unrealistic expectation in the weapons effectiveness would have resulted from the use of the GDEM data to predict the coverage percentages in the water column. The MODAS data also would have given the user a much more realistic picture of the acoustic environment for this day. The knowledge that the acoustic coverage varied slowly and that only a narrow range of coverage percentages would be observed would have been of particular importance.

B. FUTURE WORK

The most obvious limitation of this work was the limited data set. Any future work should include data that covered a wider number of areas and times. Areas of strong thermal and salinity contrast are of particular interest. Various combinations of the user supplied inputs into the WAPP should also be studied. The effects of variables such as bottom type and position (upslope/downslope) need to be addressed. Also a classified study that investigated the weapon presets themselves would be of interest. Another avenue of study is the determination of how the number of altimeters affects the accuracy of the outputs. It has been determined that the presets are sensitive to the addition of satellite data. However, the effect of the number of satellite inputs still remains to be determined. Once this is done an optimal number of altimeters can be determined based on minimizing cost and maximizing preset accuracy.

APPENDIX A INPUT HISTOGRAMS

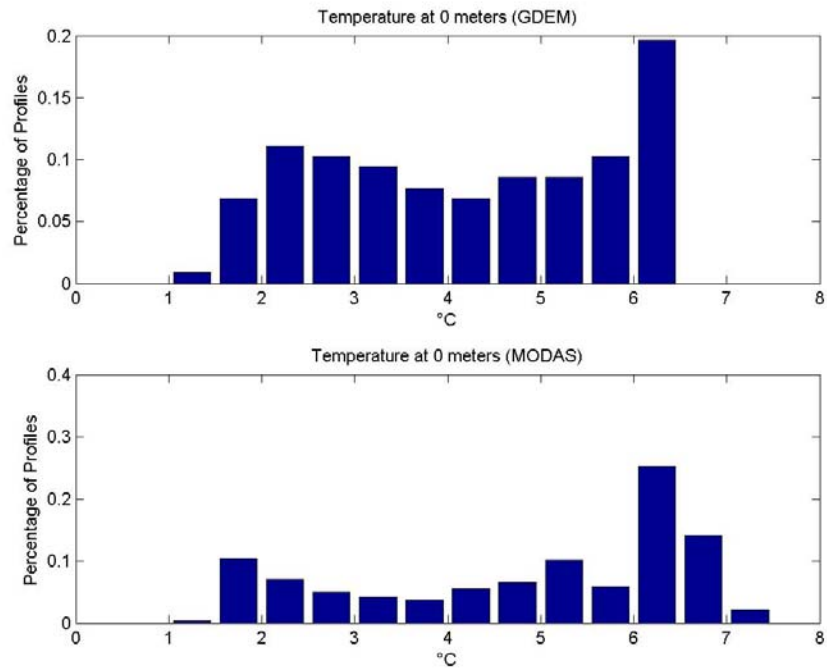


Figure 14. Temperature Distribution at 0 meters

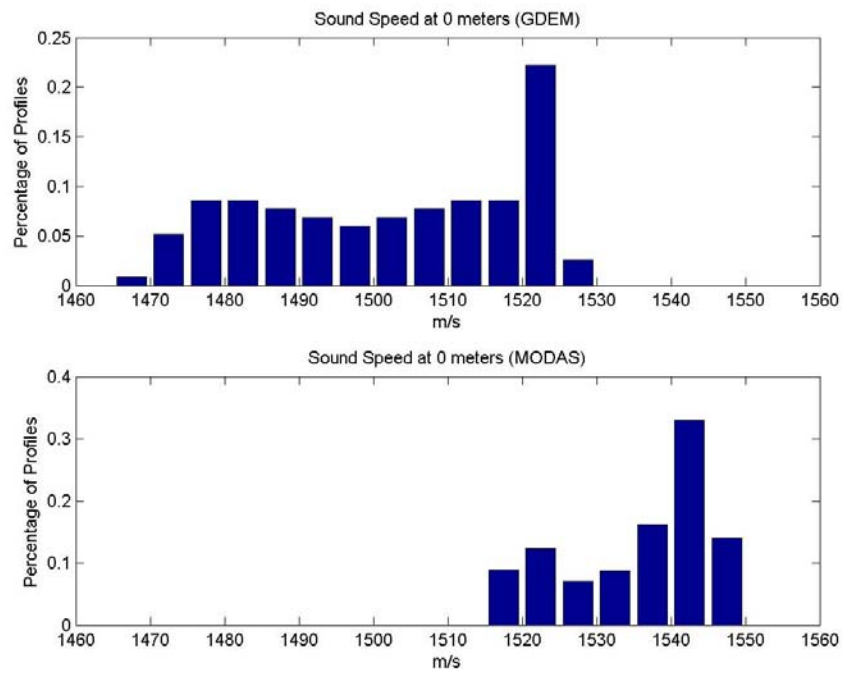


Figure 15. Salinity Distribution at 0 meters

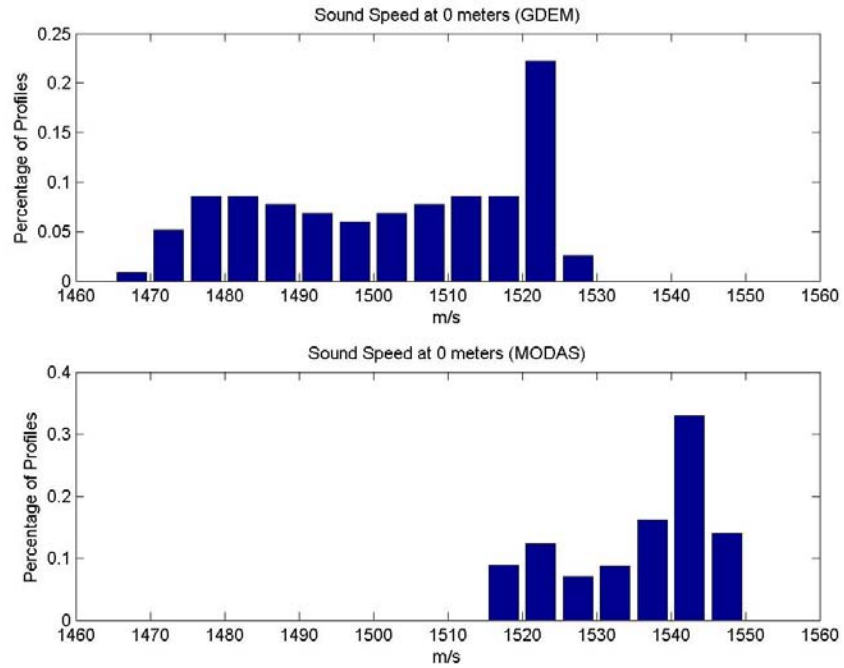


Figure 16. Sound Speed Distribution at 0 meters

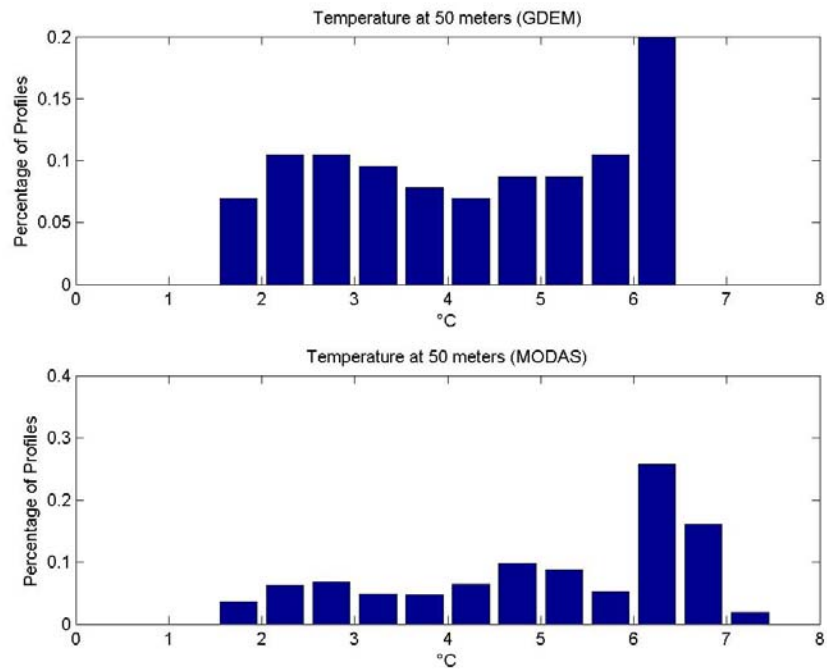


Figure 17. Temperature Distribution at 50 meters

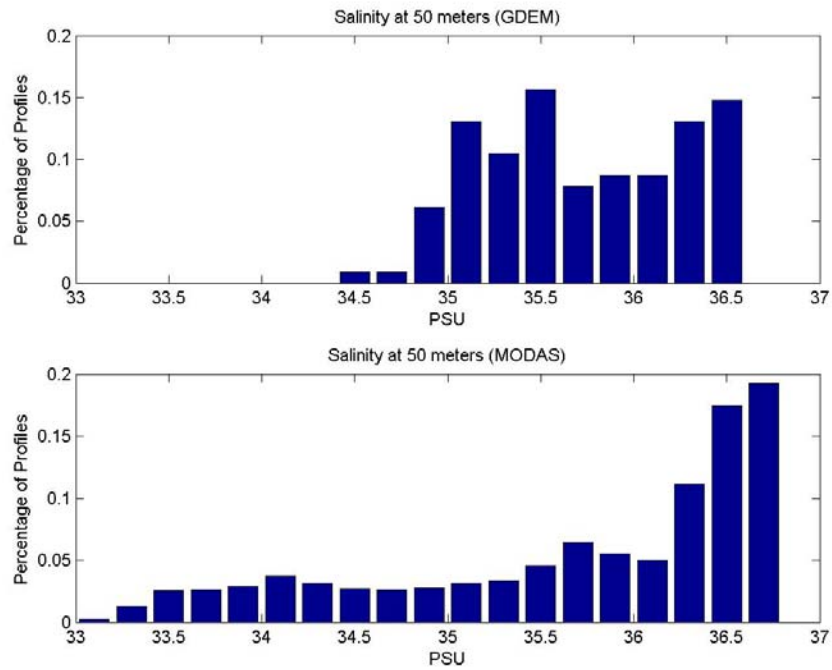


Figure 18. Salinity Distribution at 50 meters

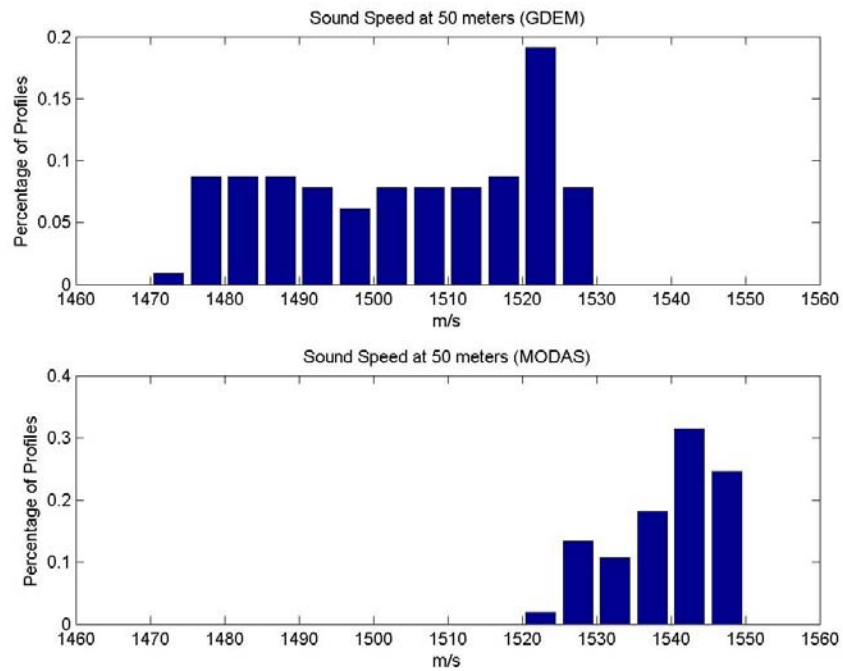


Figure 19. Sound Speed Distribution at 50 meters

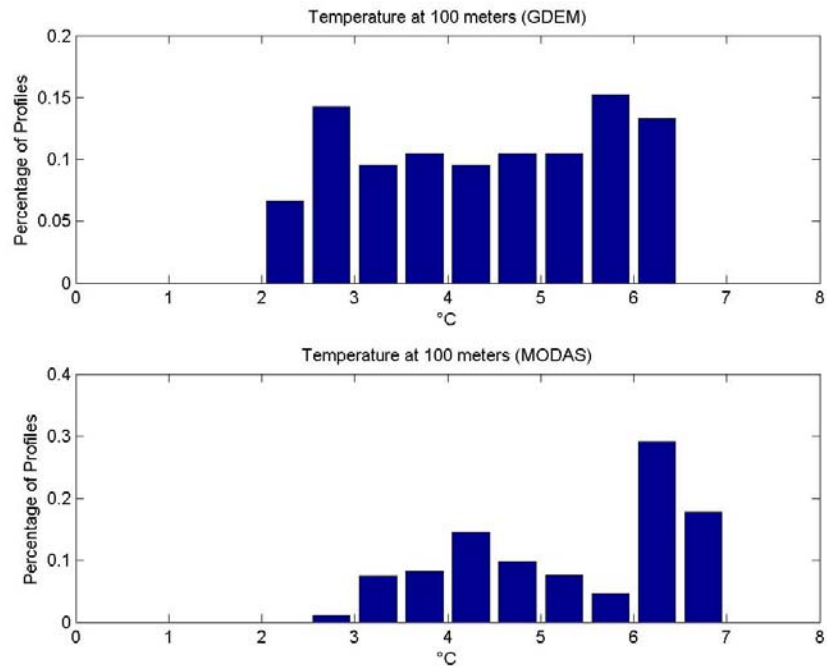


Figure 20. Temperature Distribution at 100 meters

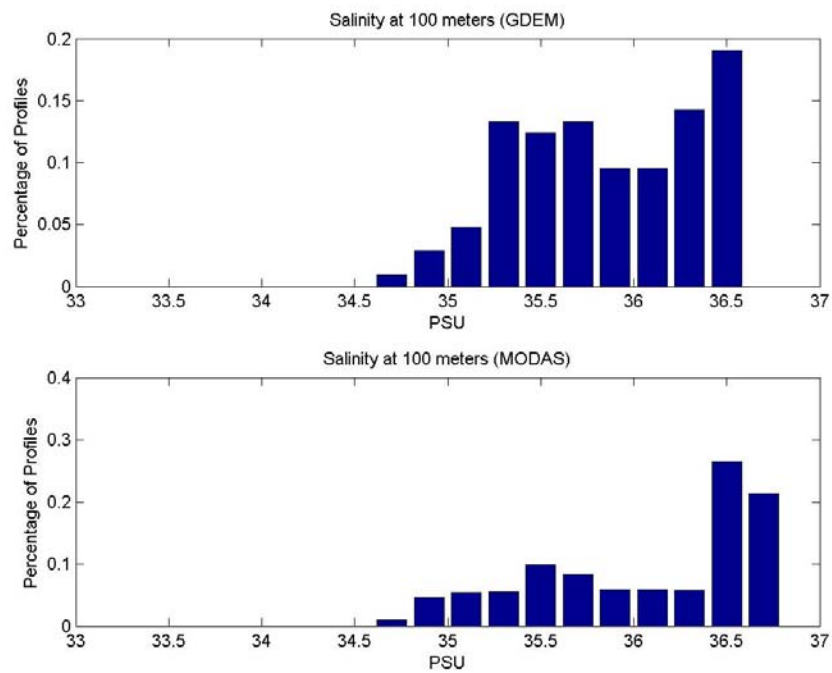


Figure 21. Salinity Distribution at 100 meters

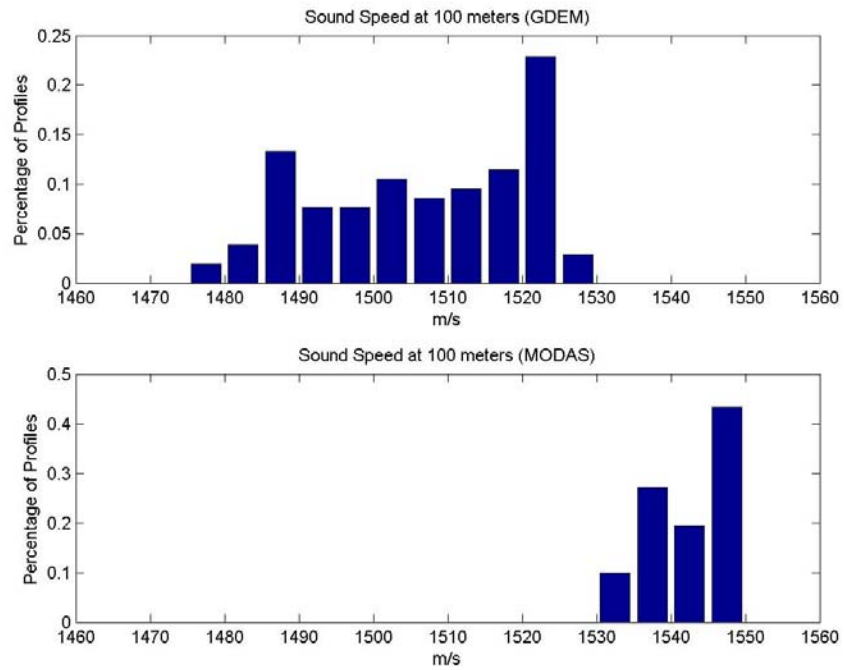


Figure 22. Sound Speed Distribution at 100 meters

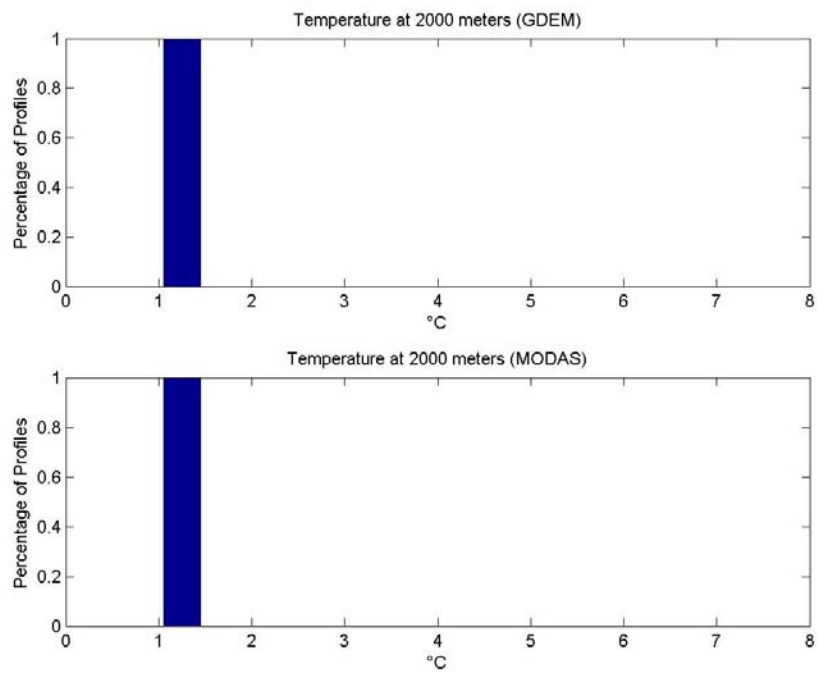


Figure 23. Temperature Distribution at 2000 meters

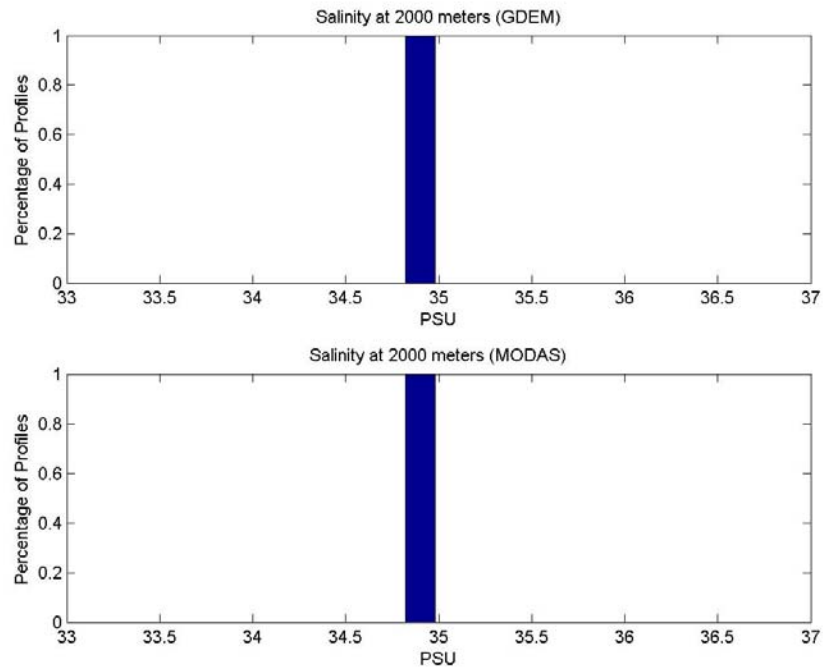


Figure 24. Salinity Distribution at 2000 meters

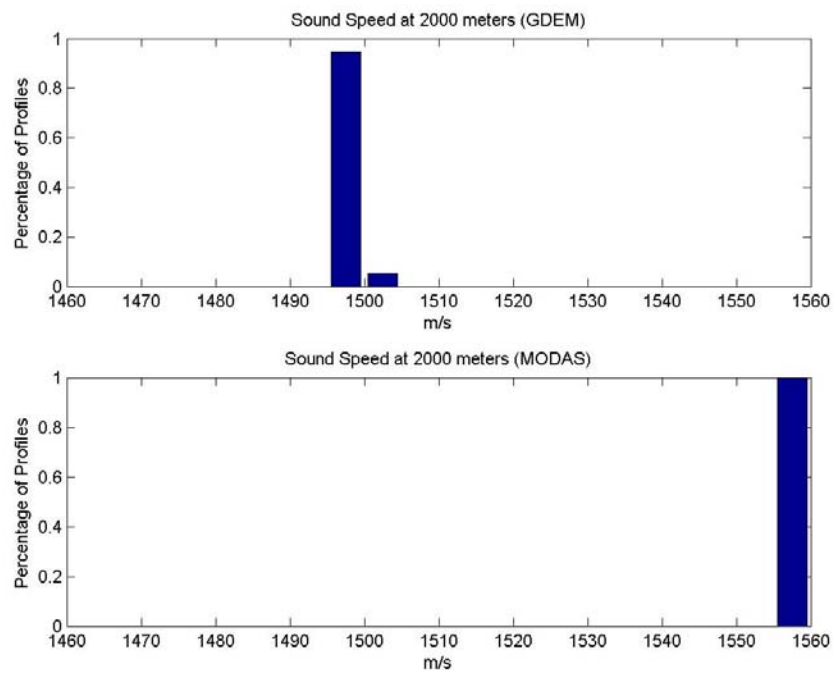


Figure 25. Sound Speed Distribution at 2000 meters

APPENDIX B INPUT RMSD GRAPHS

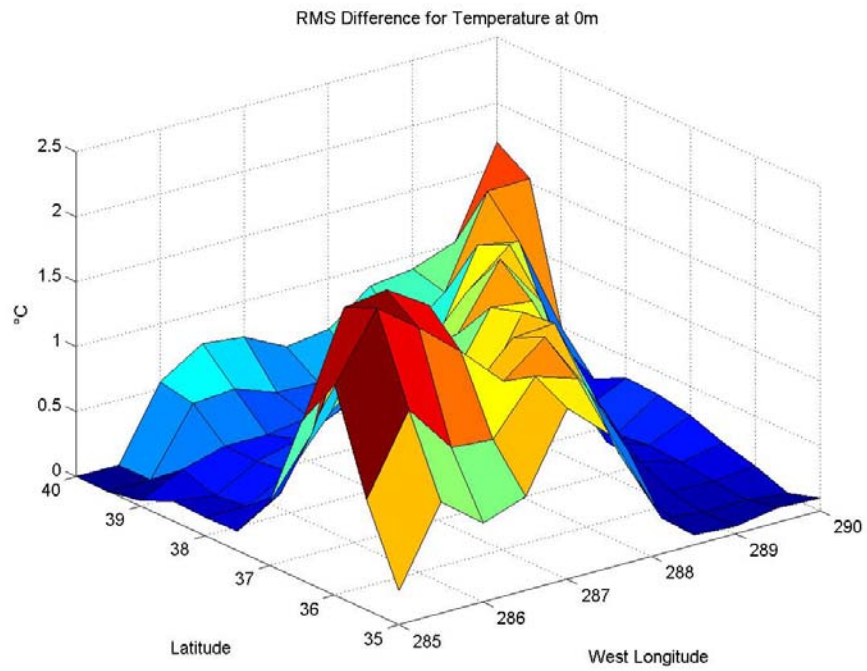


Figure 26. RMSD of Temperature at 0 meters

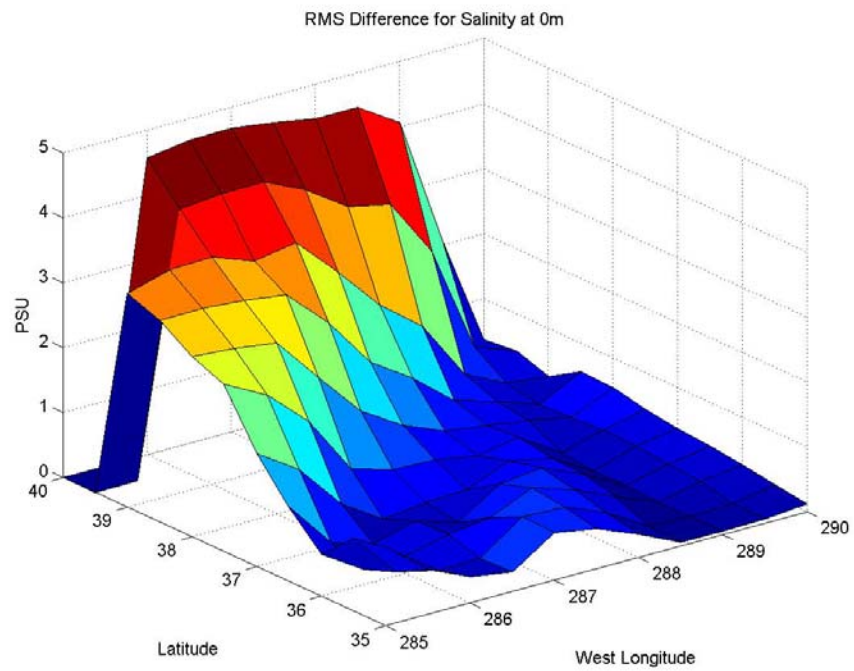


Figure 27. RMSD of Salinity at 0 meters

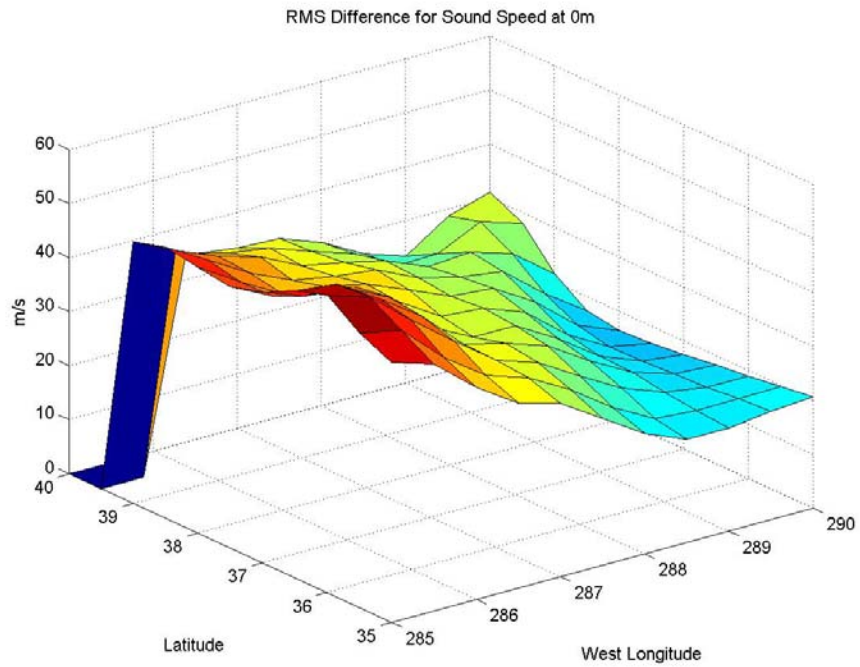


Figure 28. RMSD of Sound Speed at 0 meters

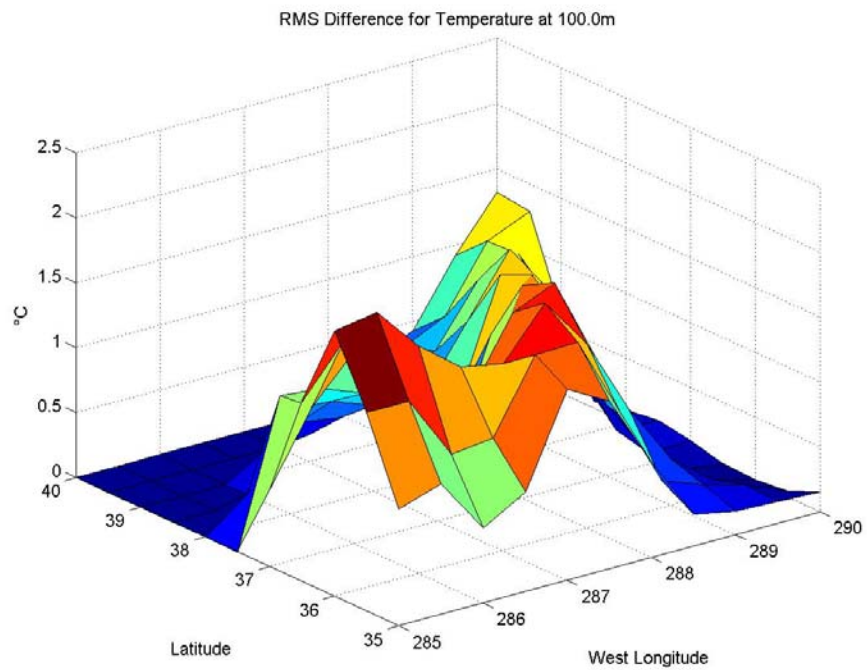


Figure 29. RMSD of Temperature at 100 meters

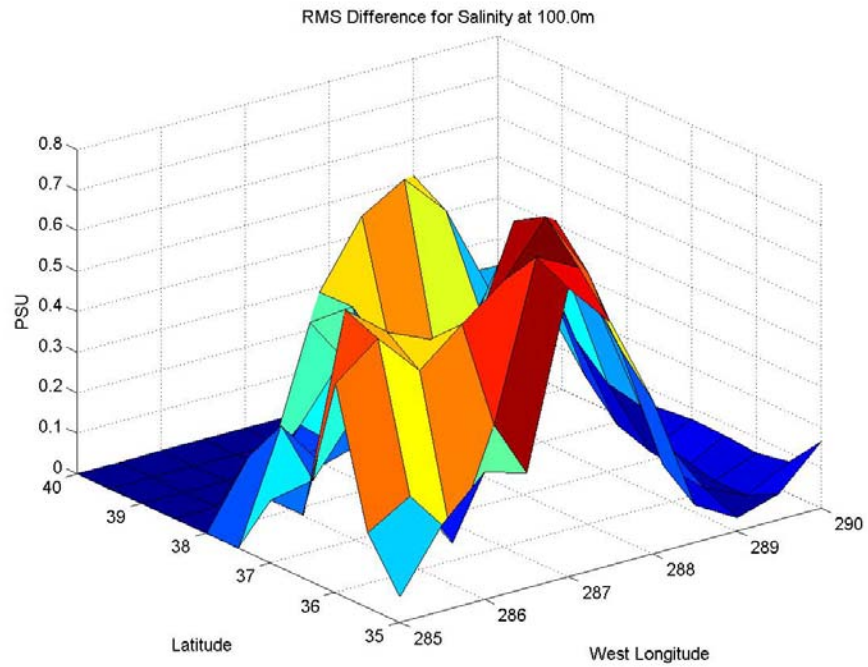


Figure 30. RMSD of Salinity at 100 meters

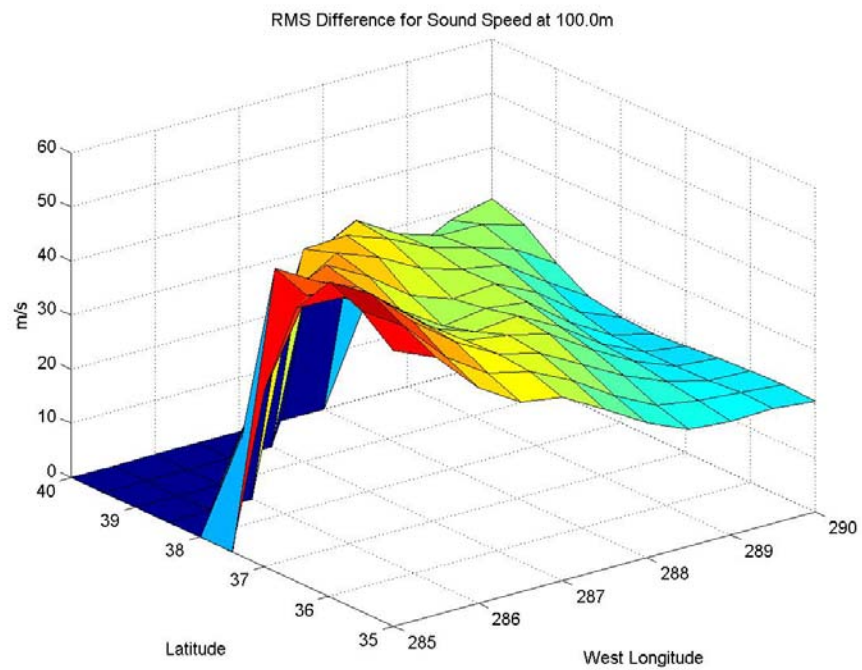


Figure 31. RMSD of Sound Speed at 100 meters

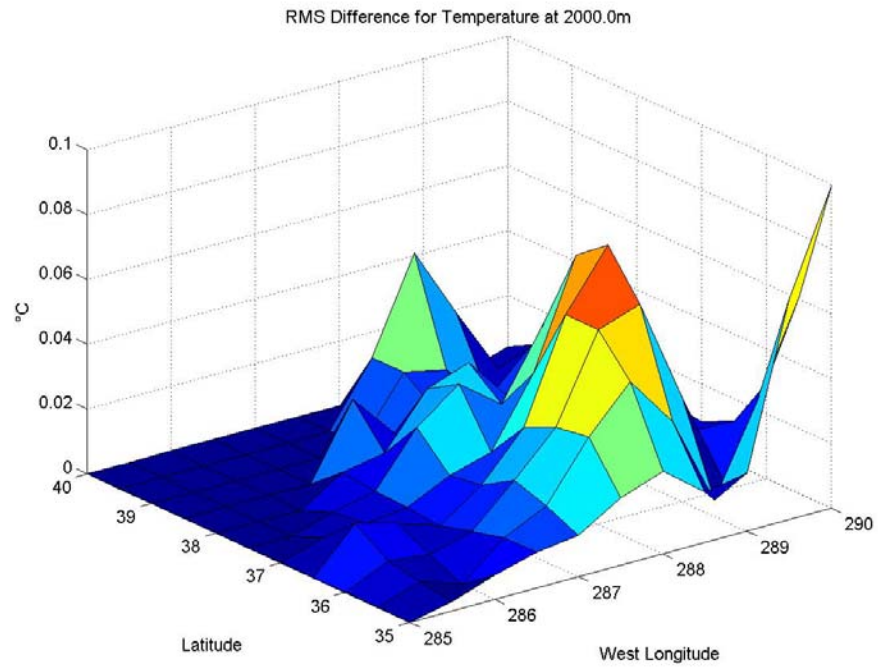


Figure 32. RMSD of Temperature at 2000 meters

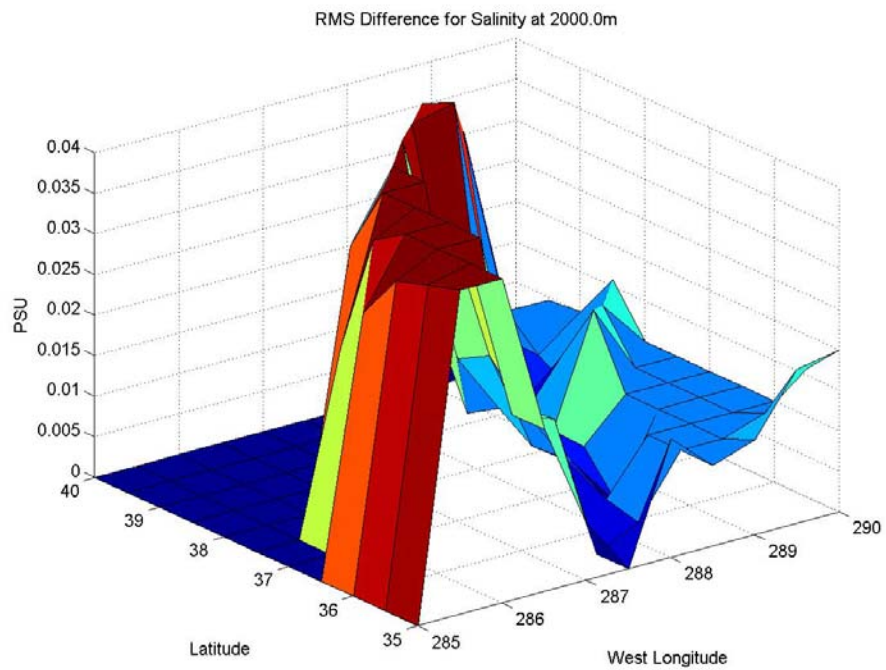


Figure 33. RMSD of Salinity at 2000 meters

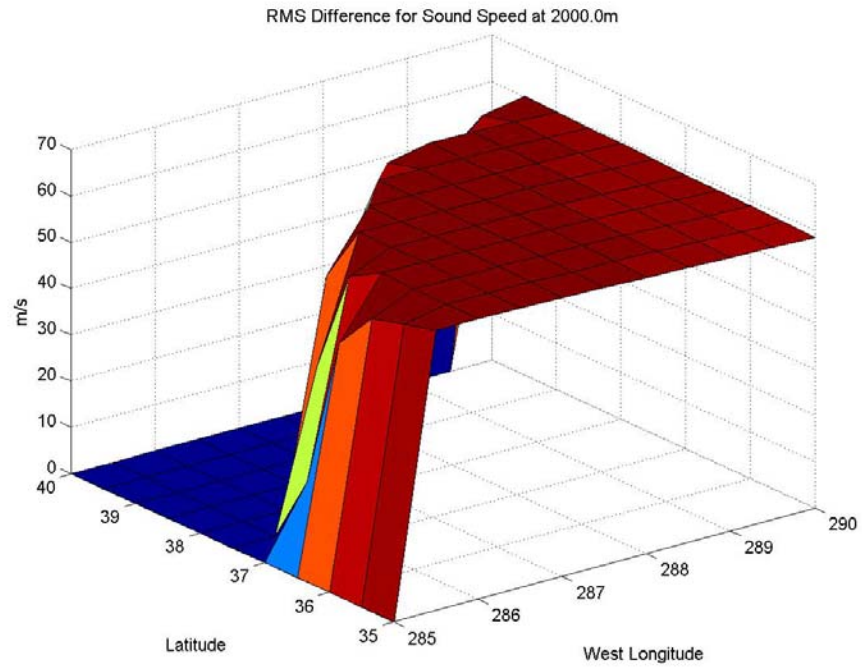


Figure 34. RMSD of Sound Speed at 2000 meters

THIS PAGE INTENTIONALLY LEFT BLANK

APPENDIX C RMSD PROFILES

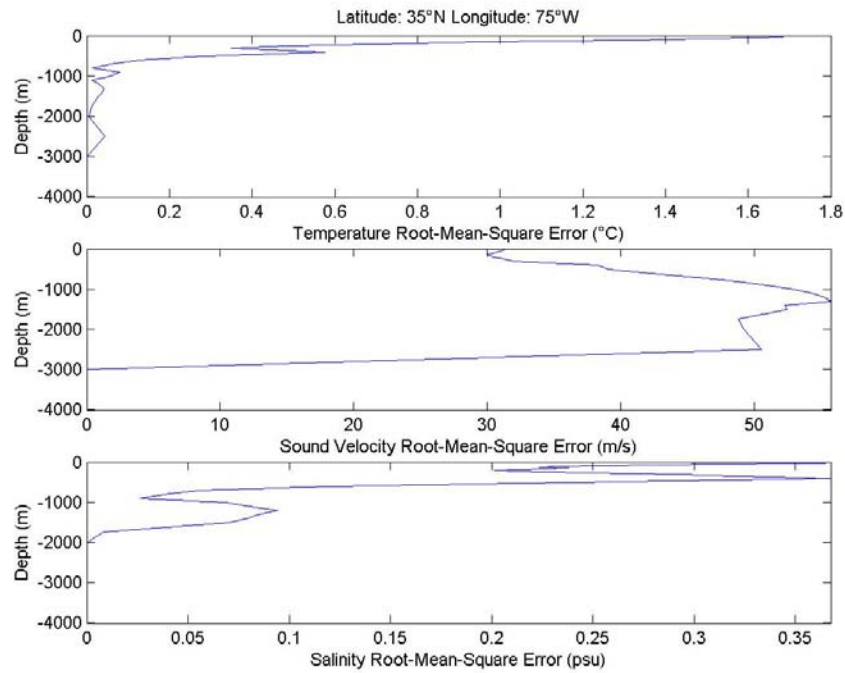


Figure 35. RMSD Profile

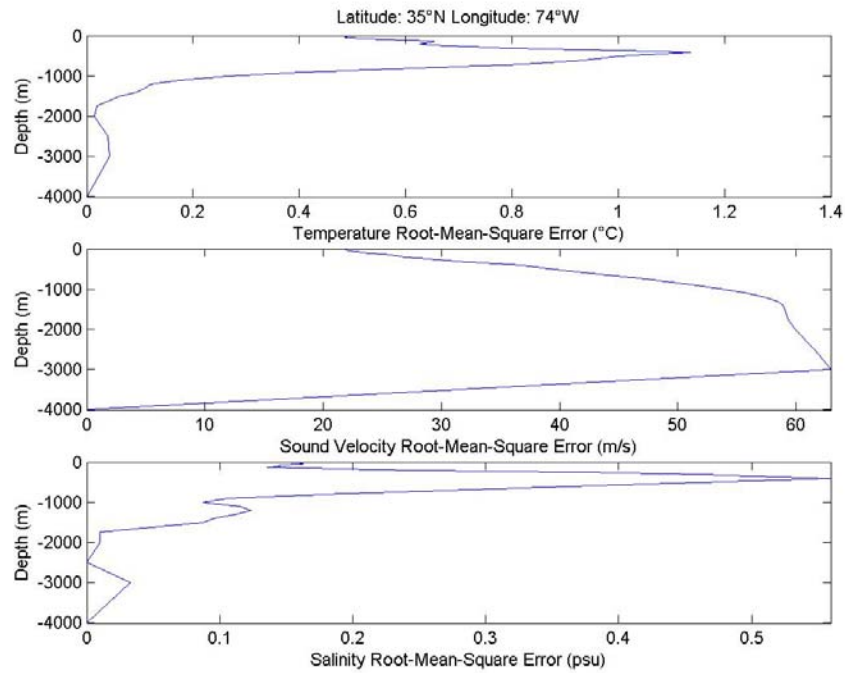


Figure 36. RMSD Profile

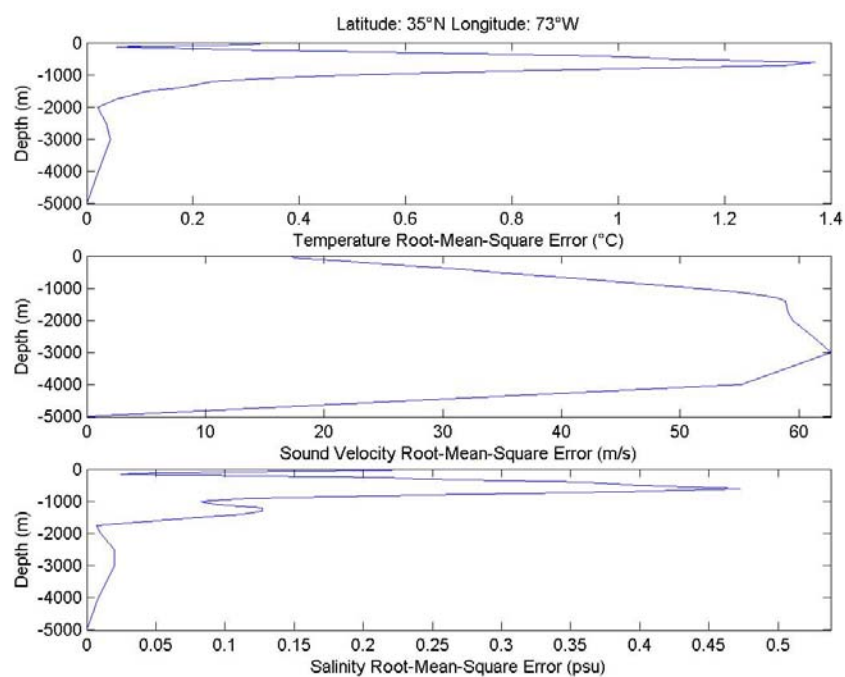


Figure 37. RMSD Profile

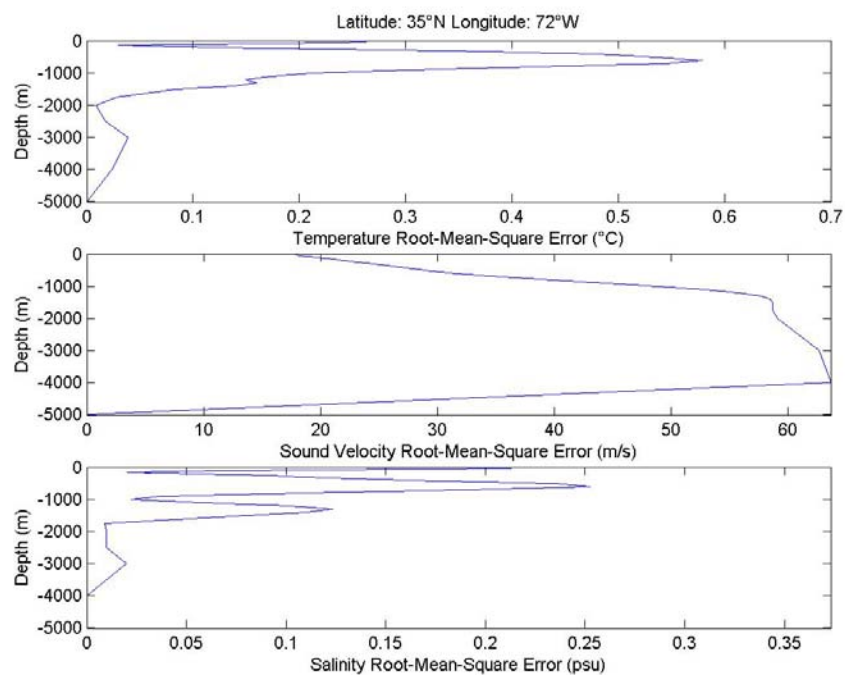


Figure 38. RMSD Profile

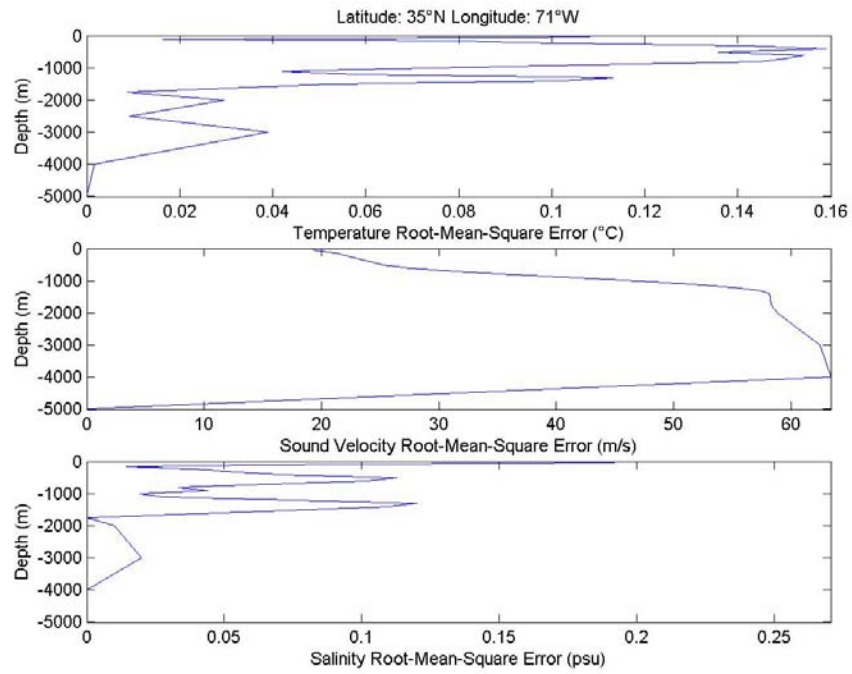


Figure 39. RMSD Profile

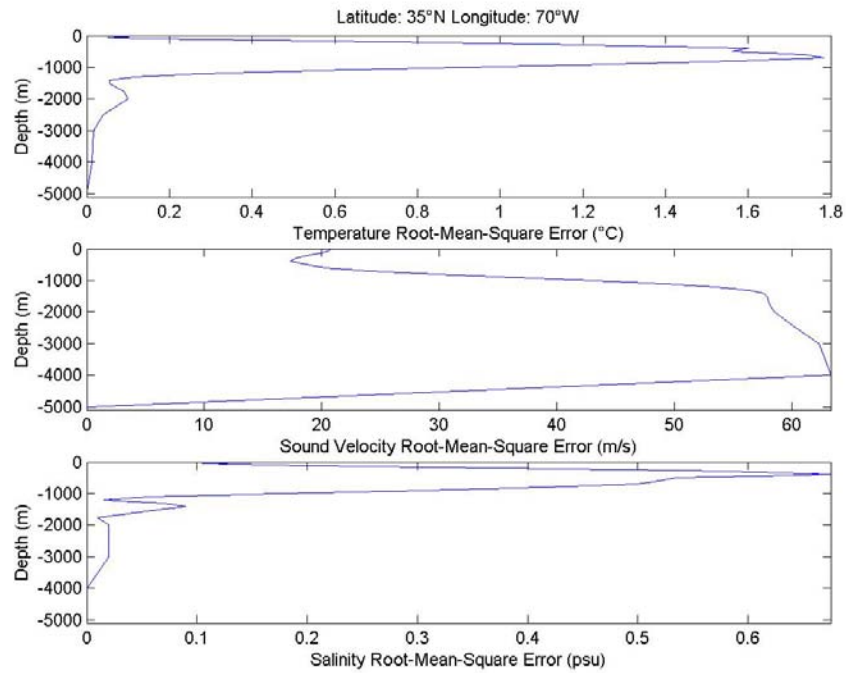


Figure 40. RMSD Profile

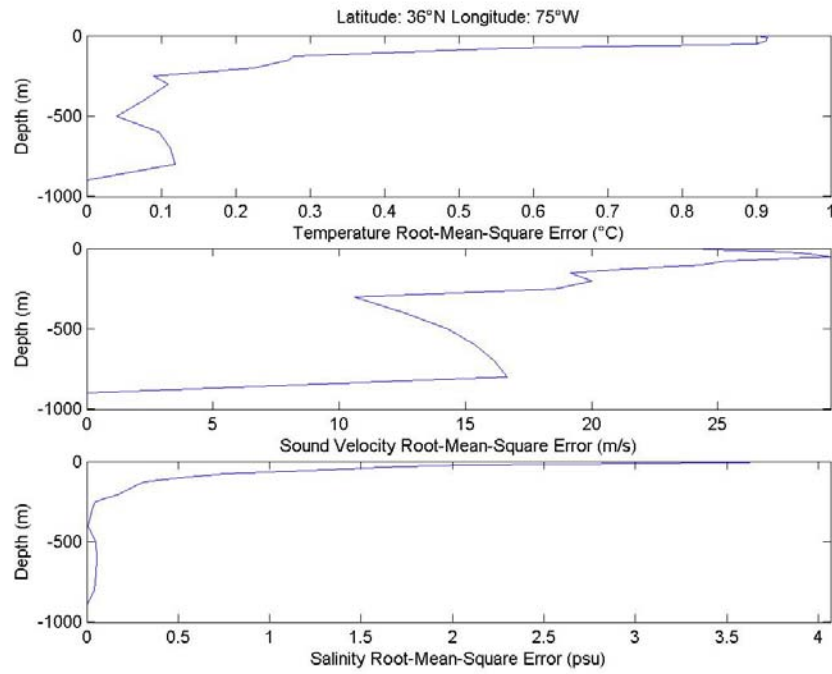


Figure 41. RMSD Profile

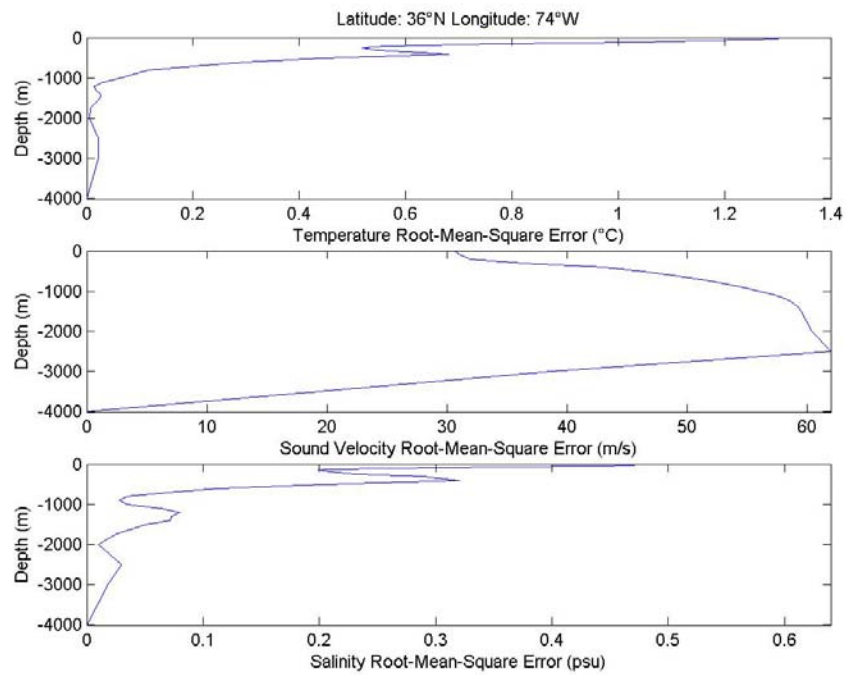


Figure 42. RMSD Profile

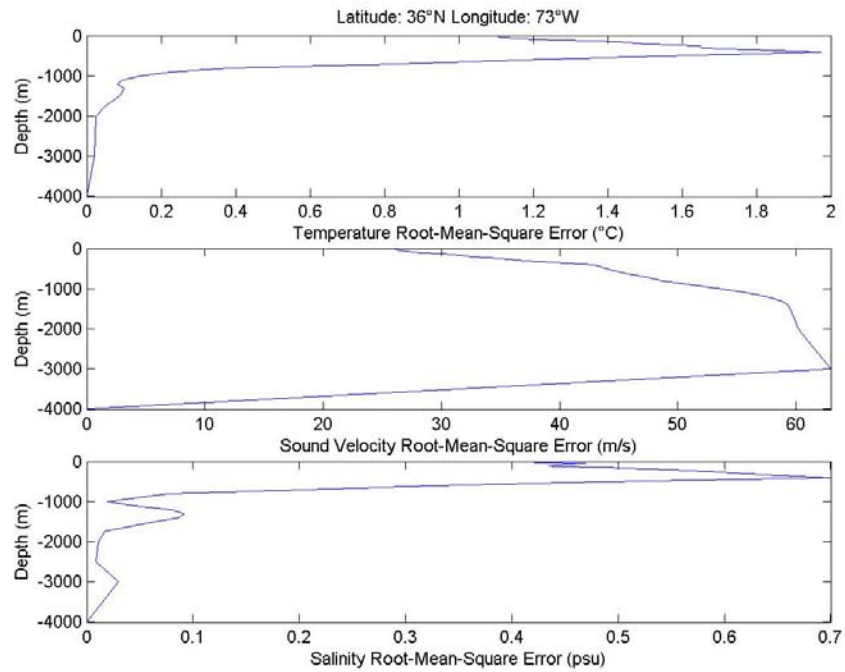


Figure 43. RMSD Profile

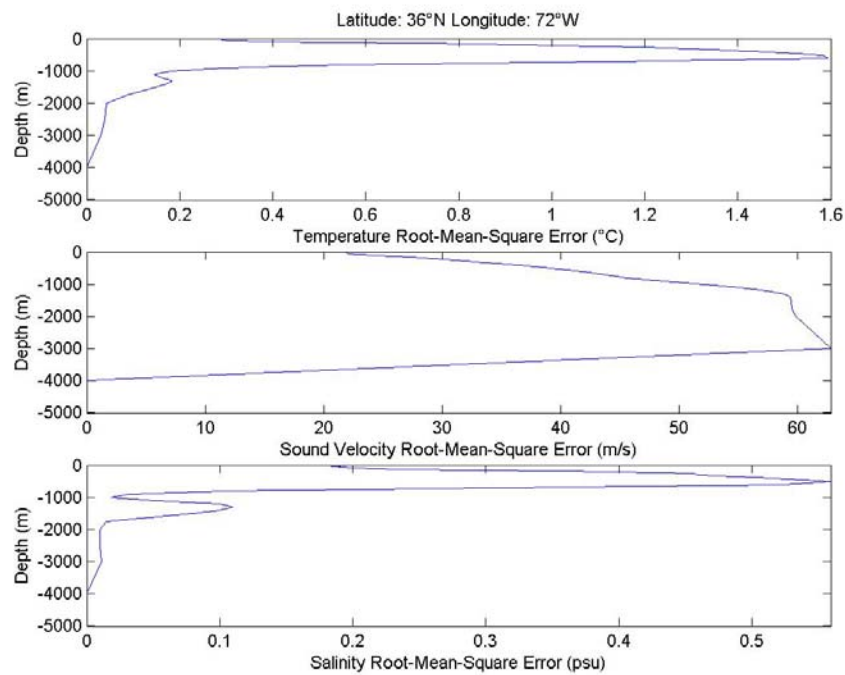


Figure 44. RMSD Profile

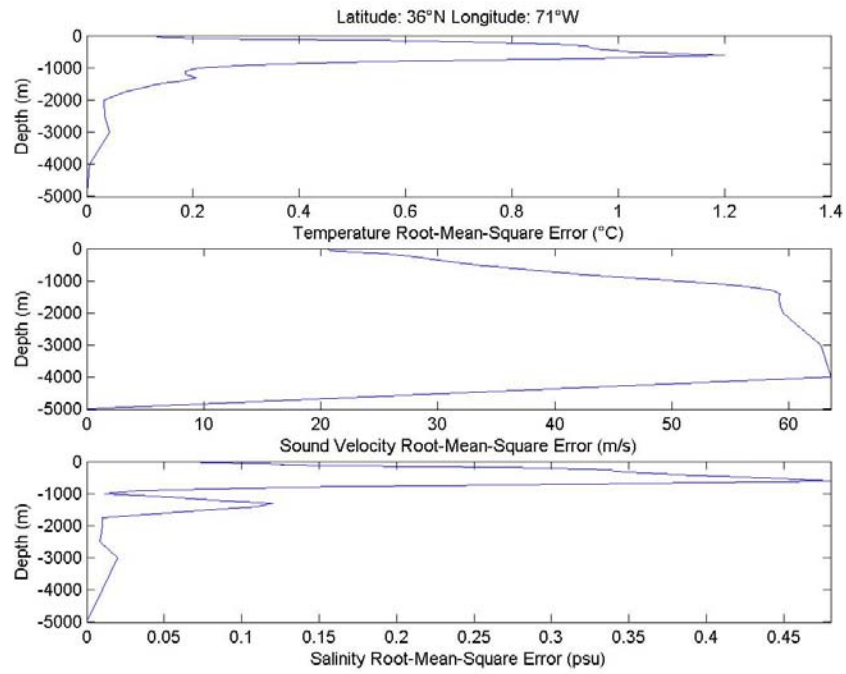


Figure 45. RMSD Profile

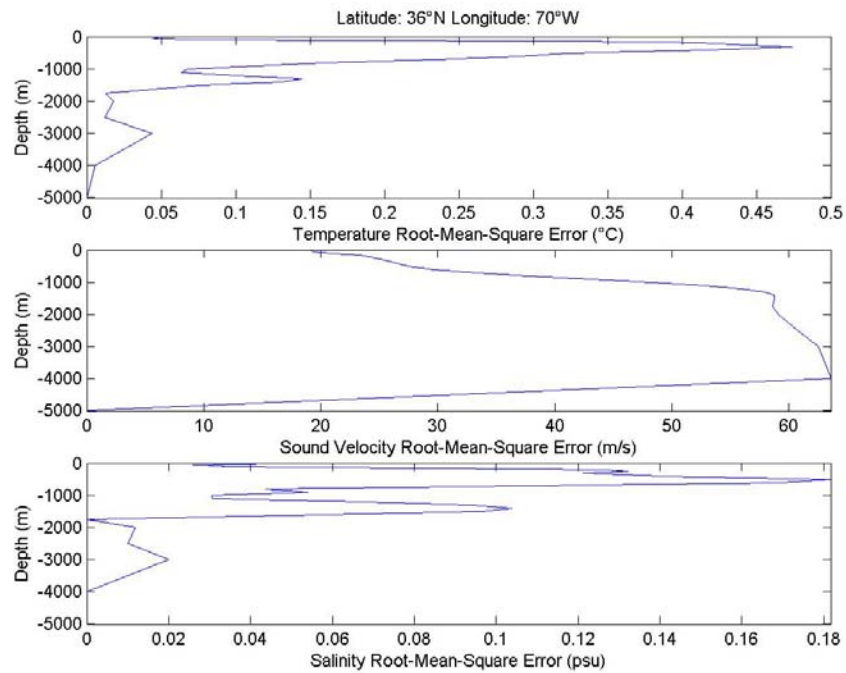


Figure 46. RMSD Profile

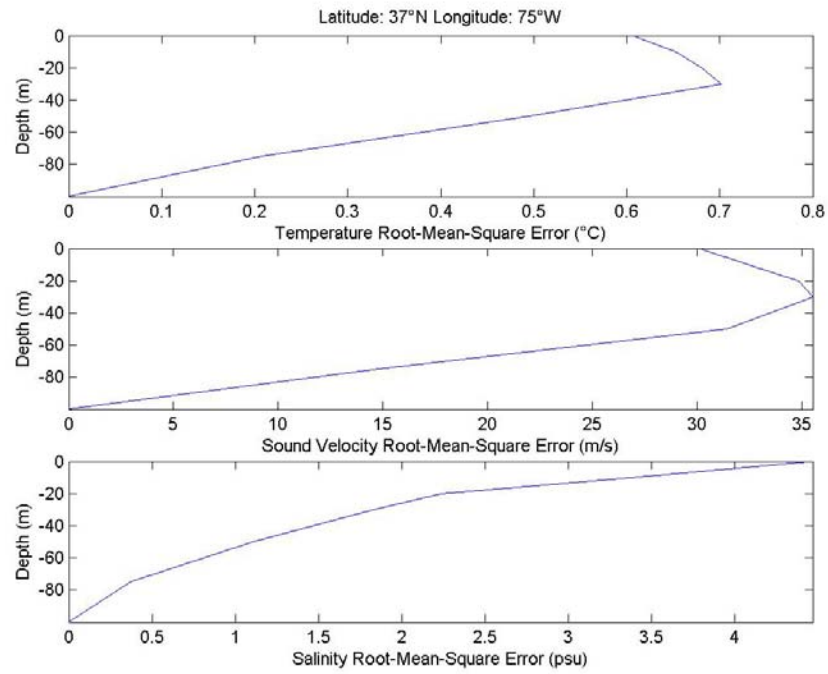


Figure 47. RMSD Profile

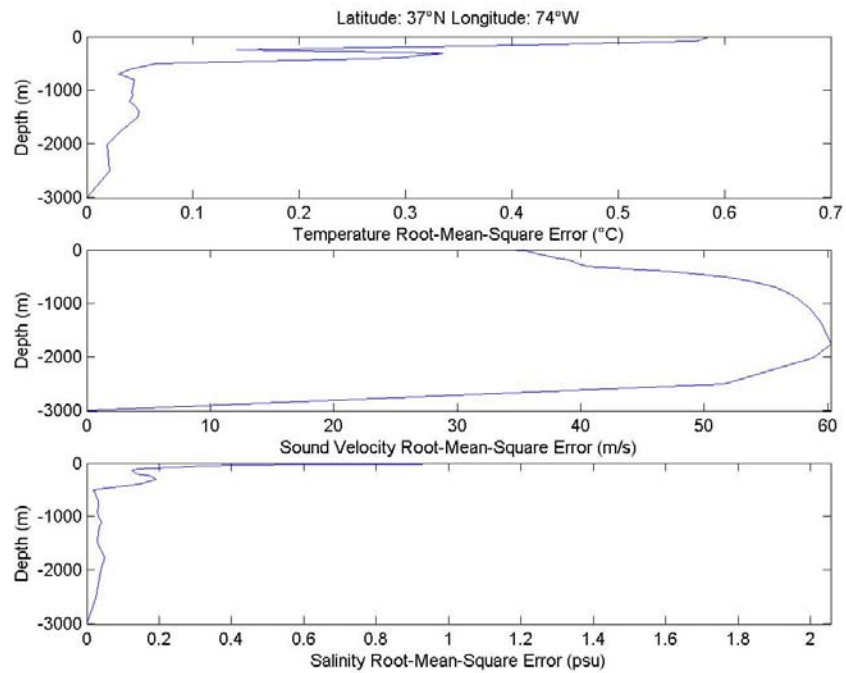


Figure 48. RMSD Profile

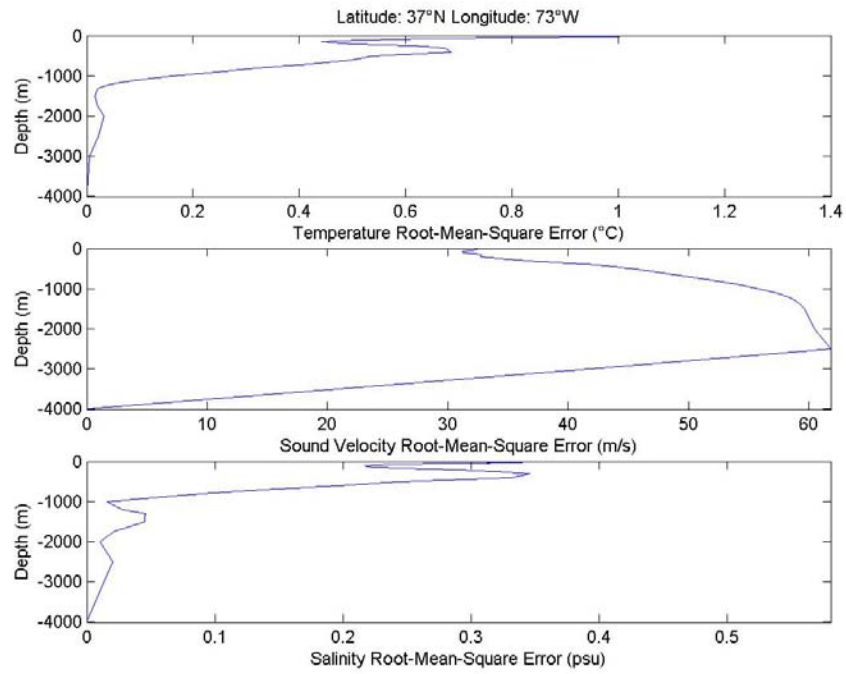


Figure 49. RMSD Profile

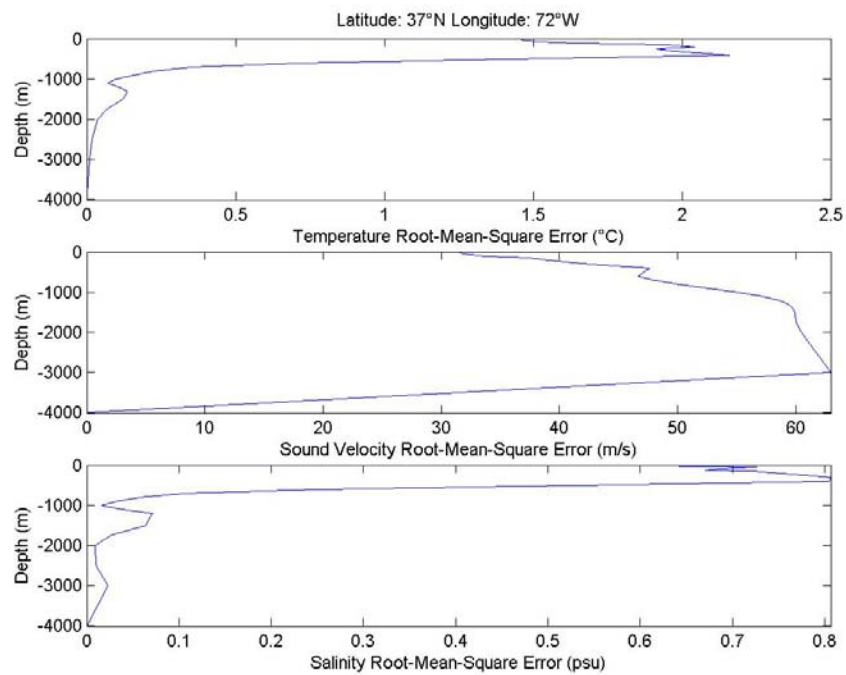


Figure 50. RMSD Profile

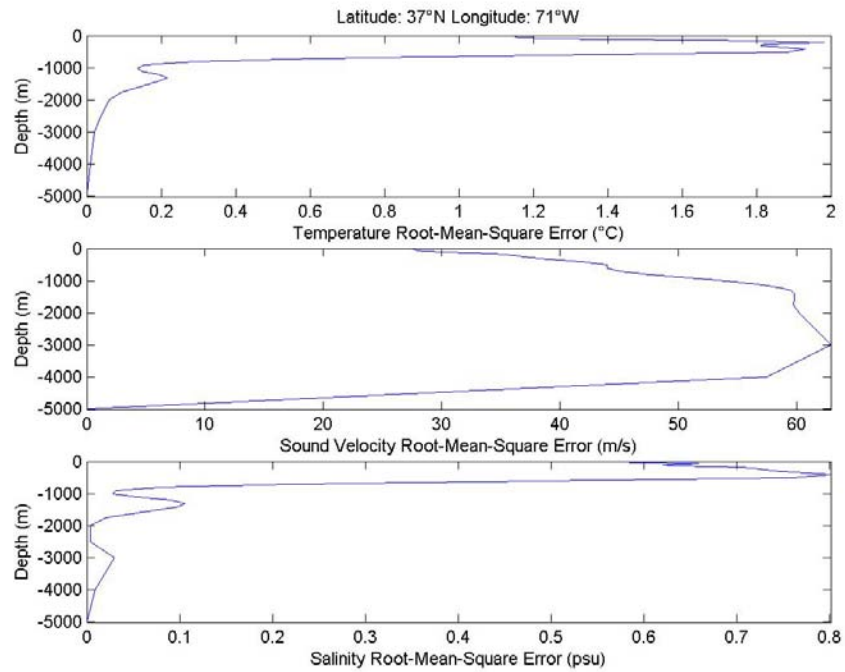


Figure 51. RMSD Profile

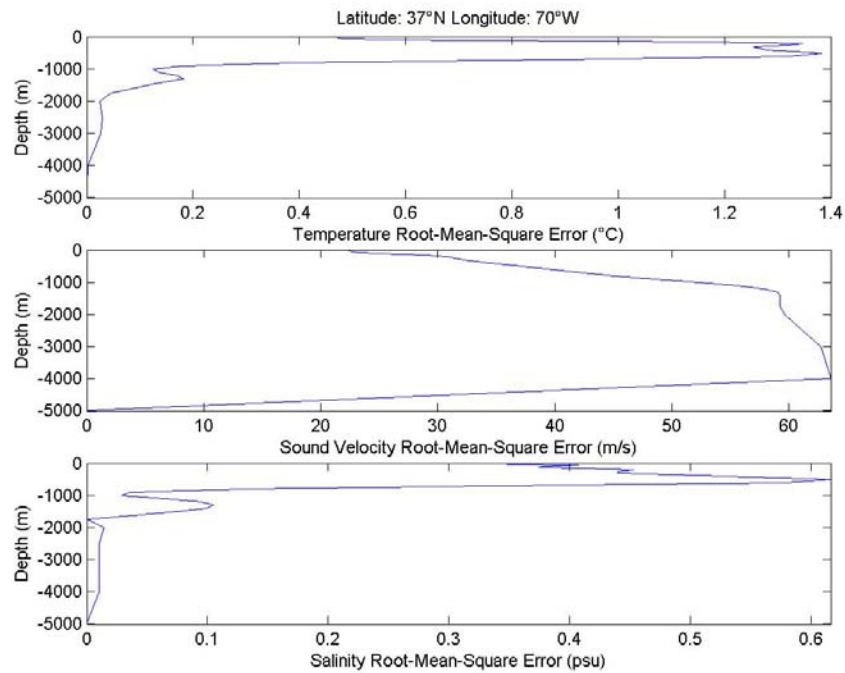


Figure 52. RMSD Profile

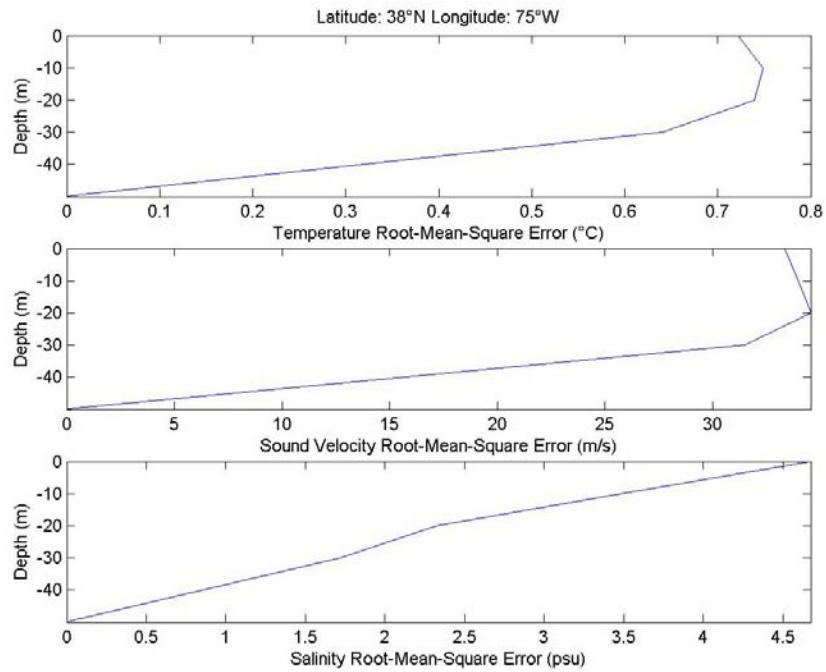


Figure 53. RMSD Profile

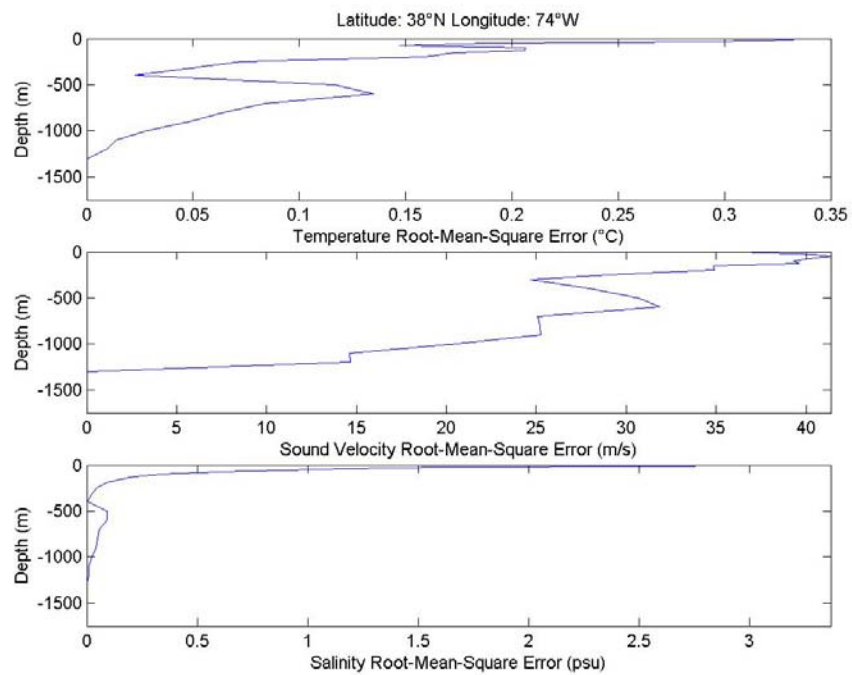


Figure 54. RMSD Profile

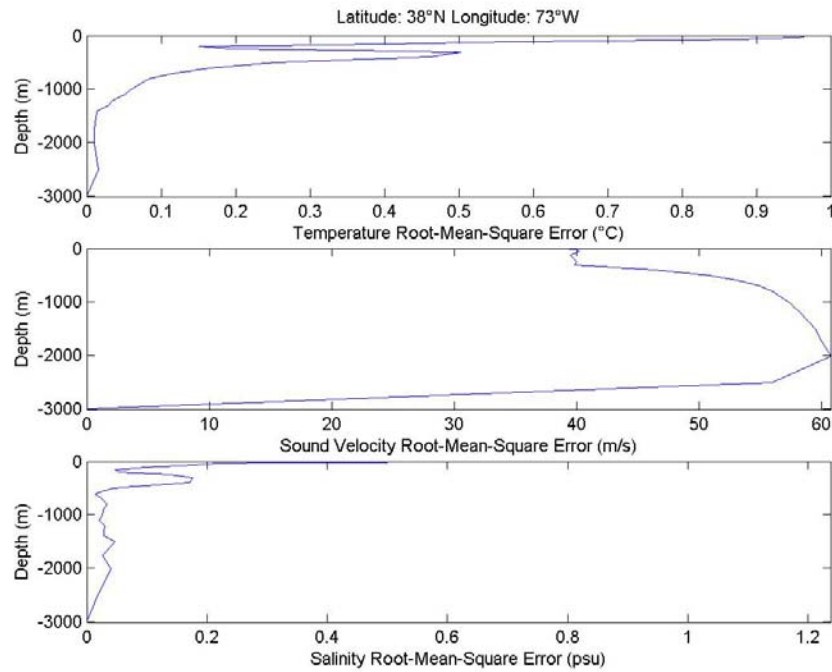


Figure 55. RMSD Profile

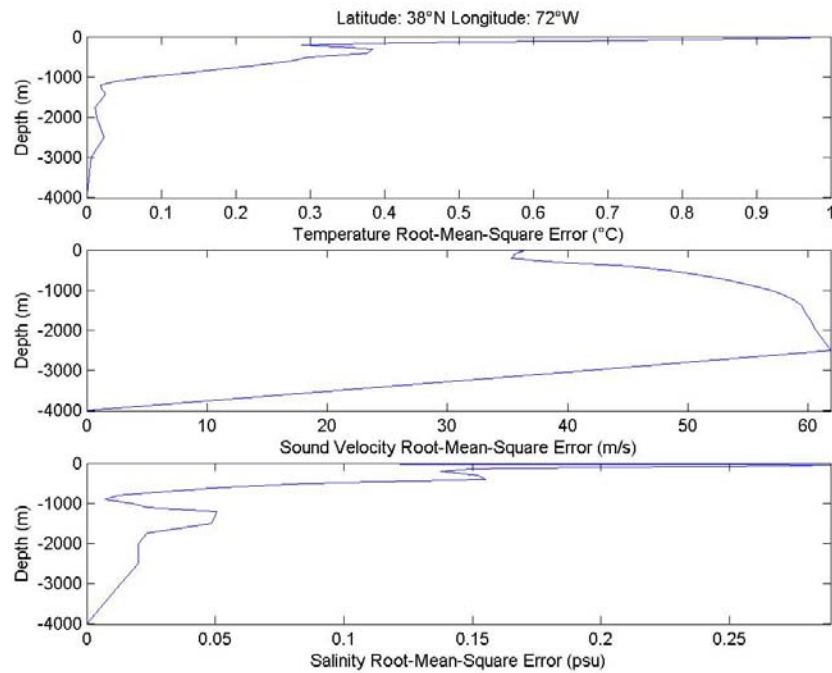


Figure 56. RMSD Profile

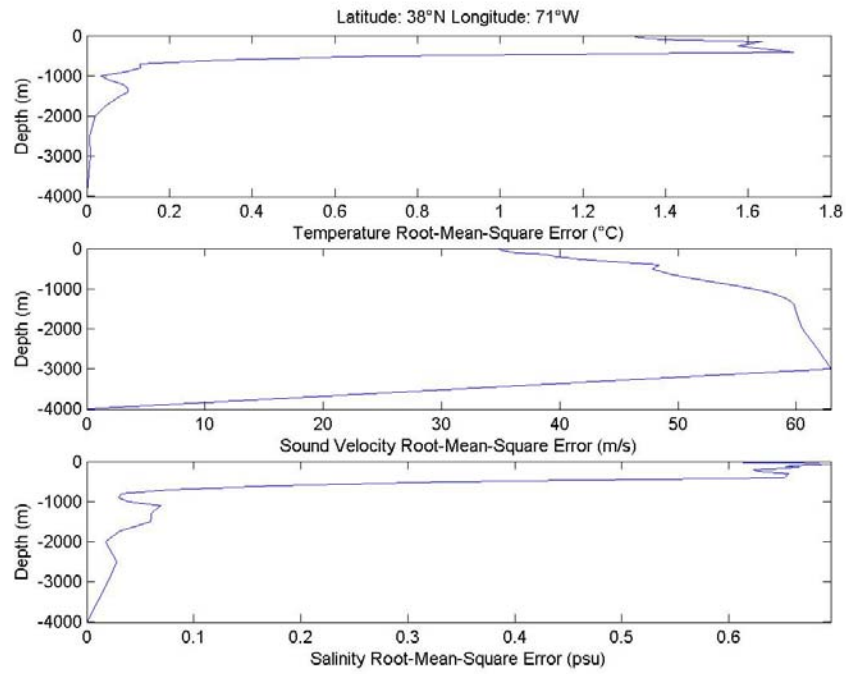


Figure 57. RMSD Profile

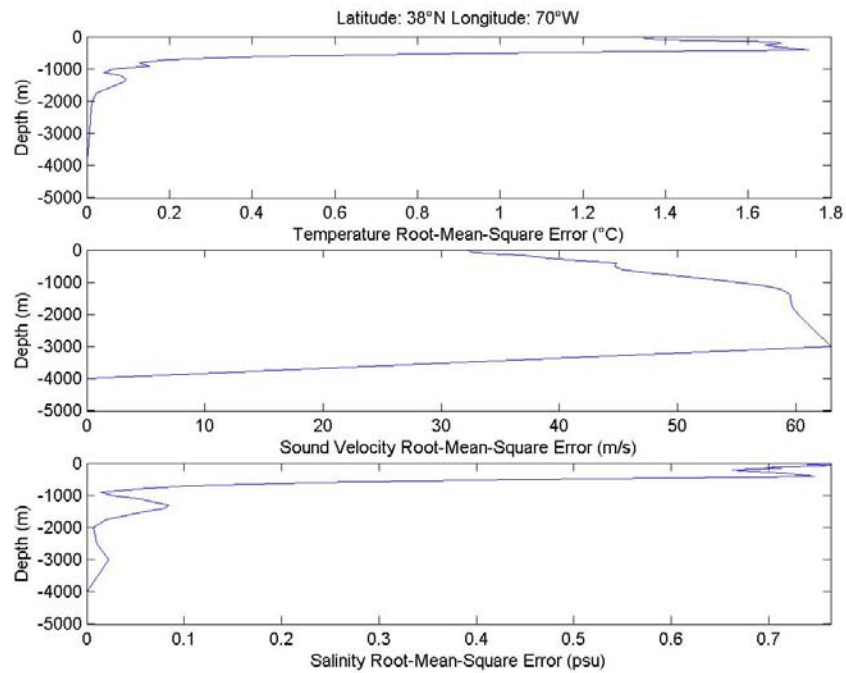


Figure 58. RMSD Profile

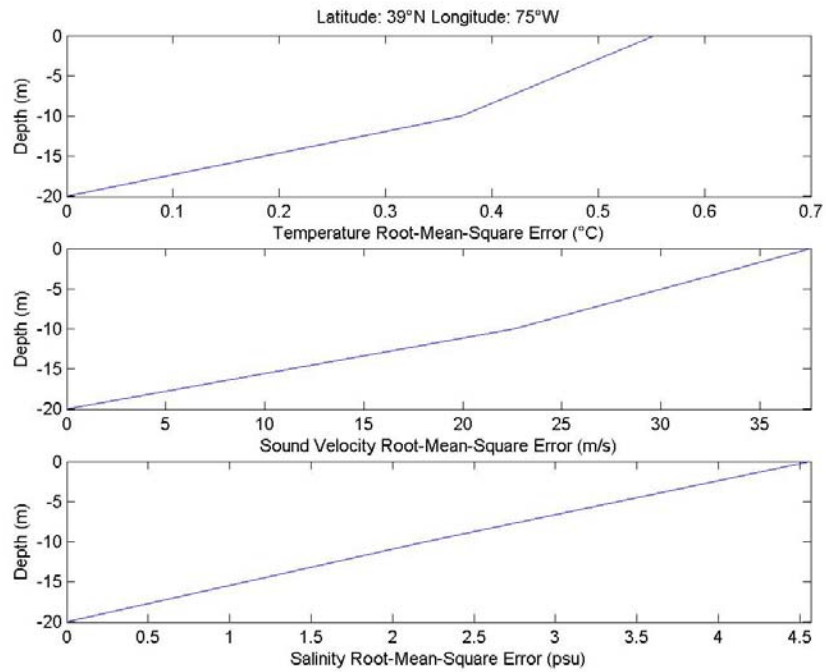


Figure 59. RMSD Profile

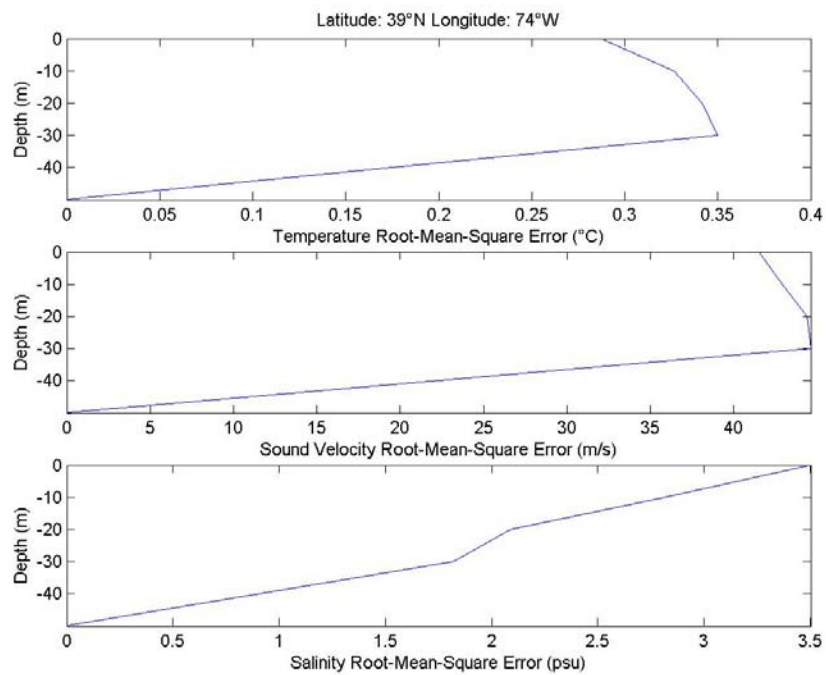


Figure 60. RMSD Profile

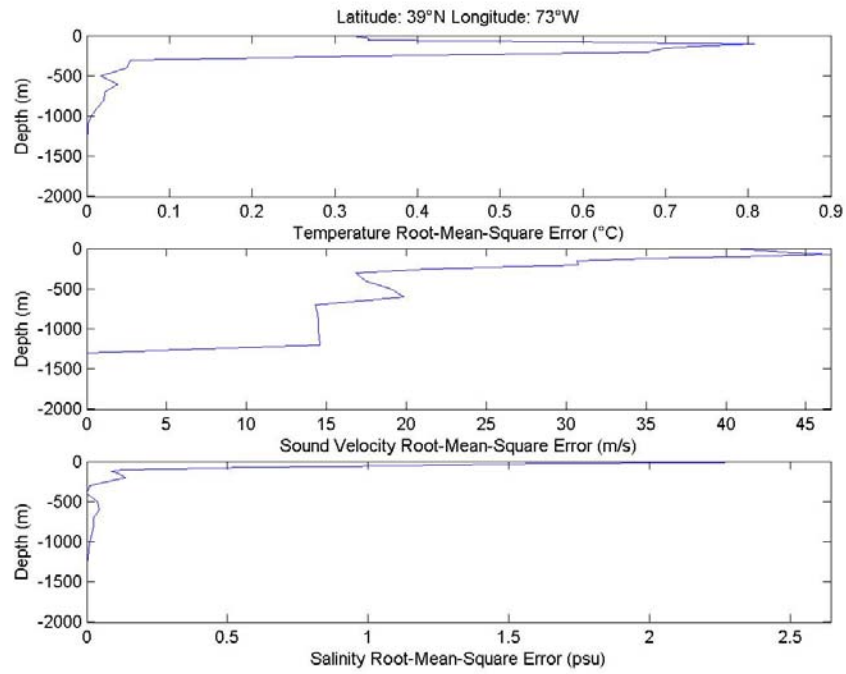


Figure 61. RMSD Profile

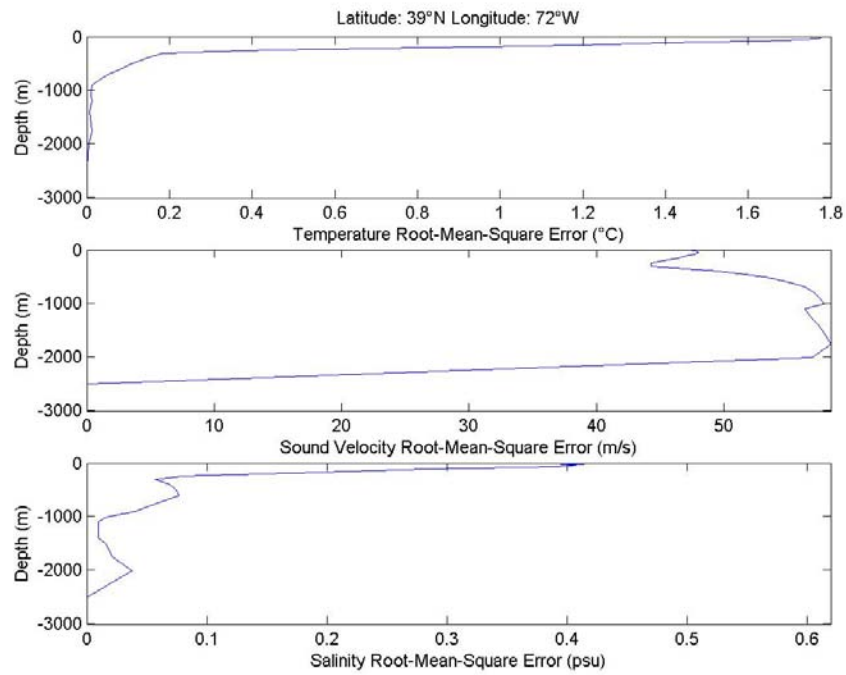


Figure 62. RMSD Profile

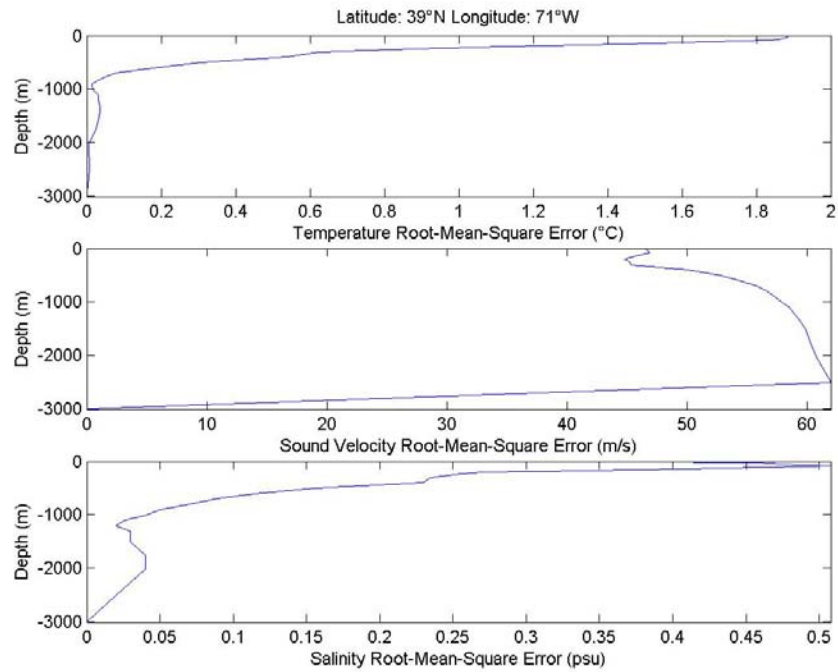


Figure 63. RMSD Profile

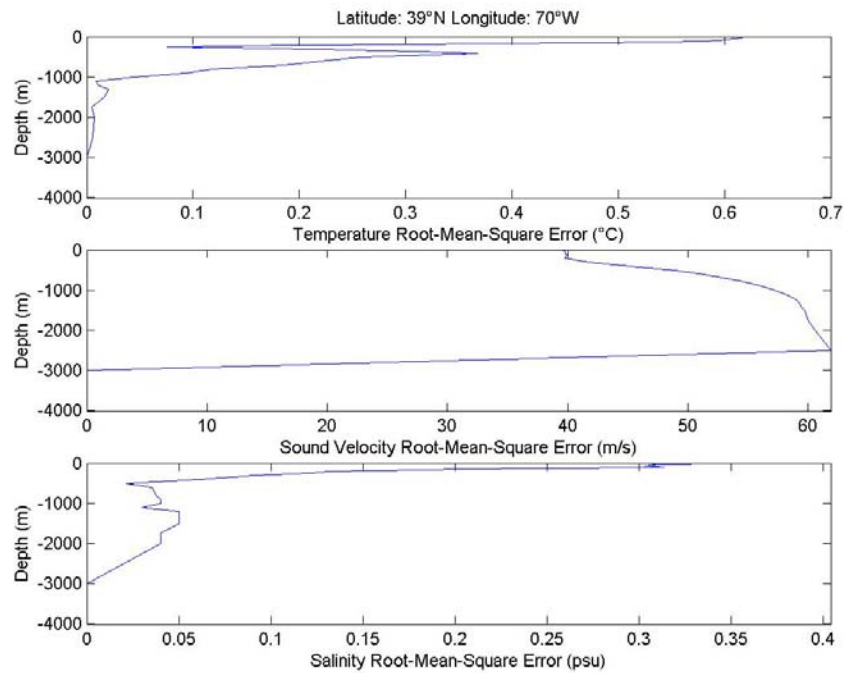


Figure 64. RMSD Profile

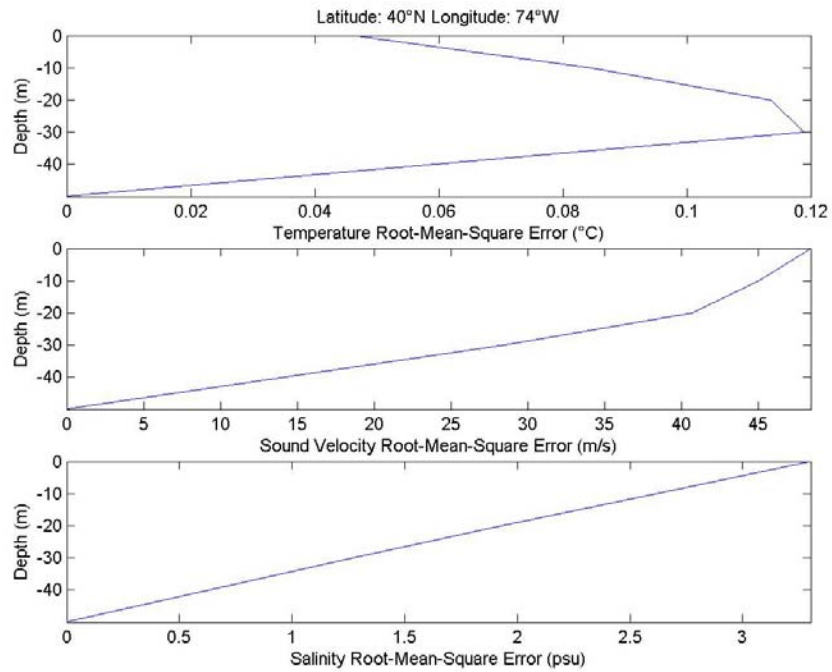


Figure 65. RMSD Profile

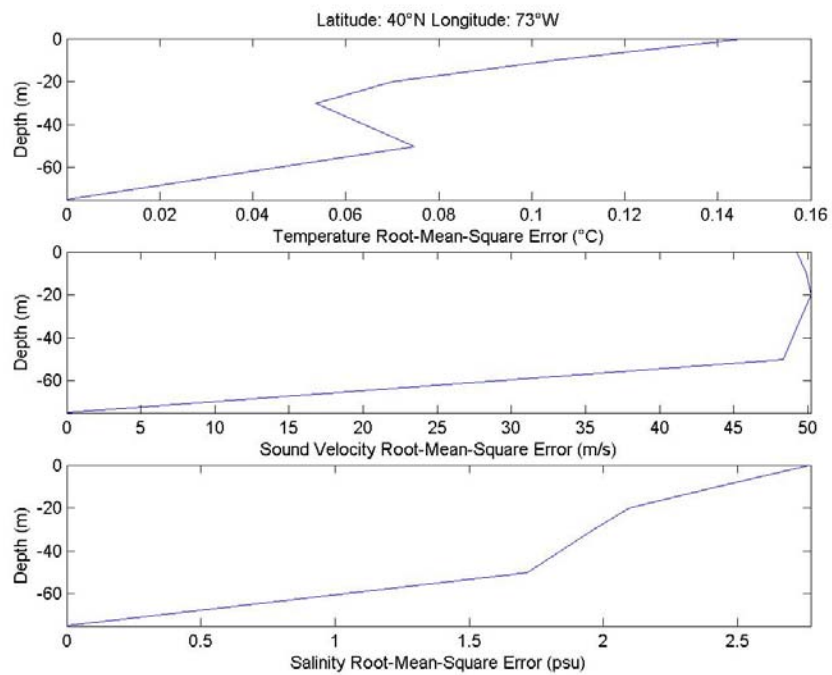


Figure 66. RMSD Profile

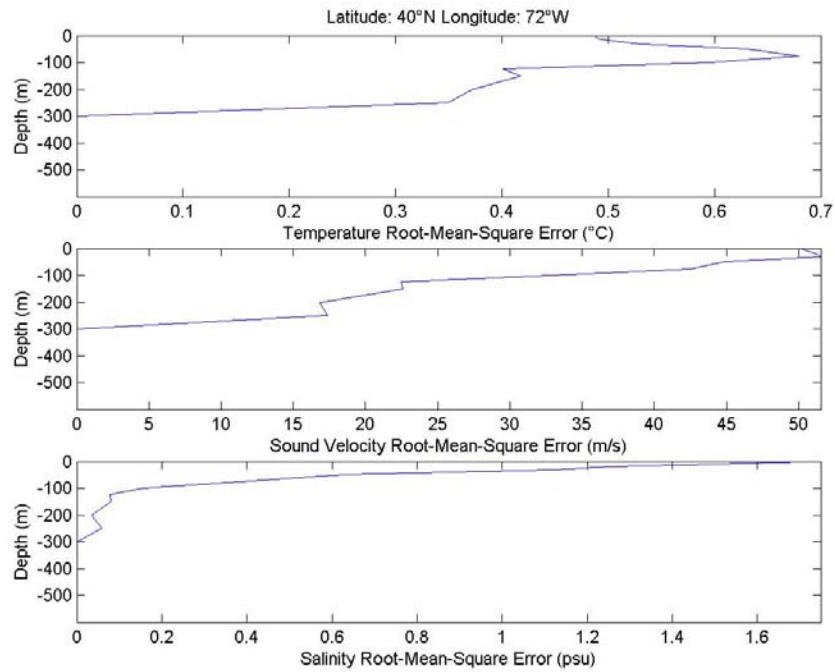


Figure 67. RMSD Profile

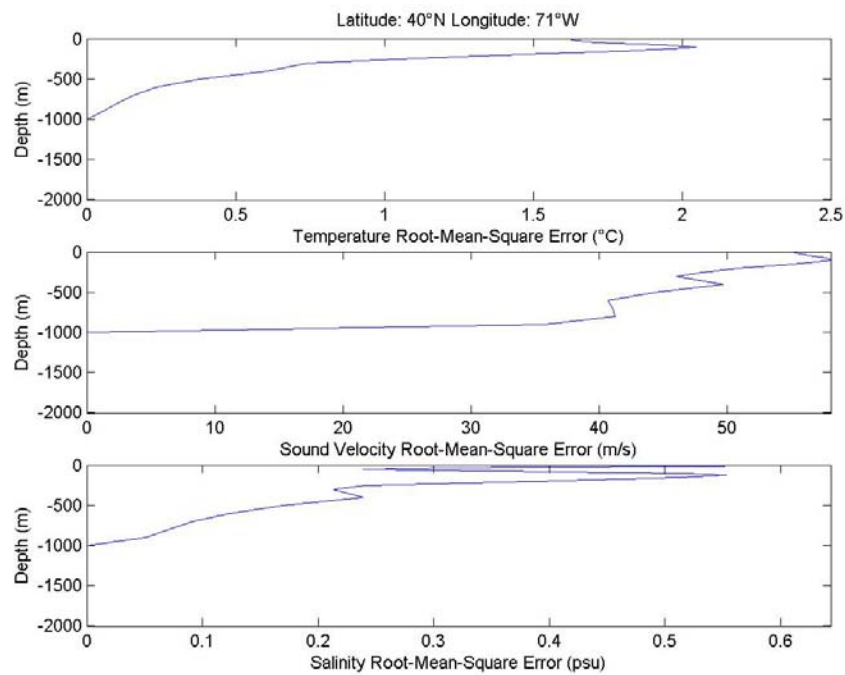


Figure 68. RMSD Profile

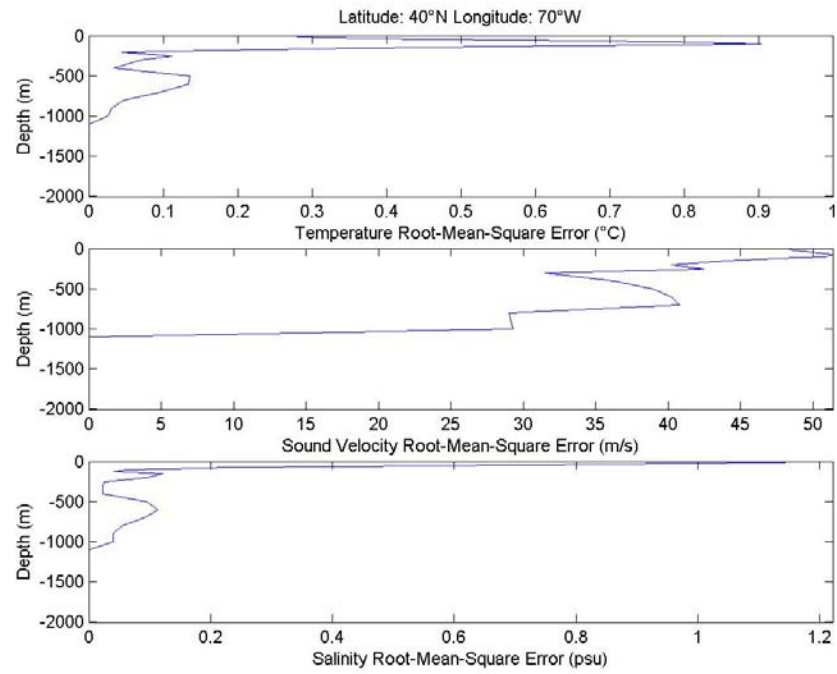


Figure 69. RMSD Profile

APPENDIX D OUTPUT HISTOGRAMS

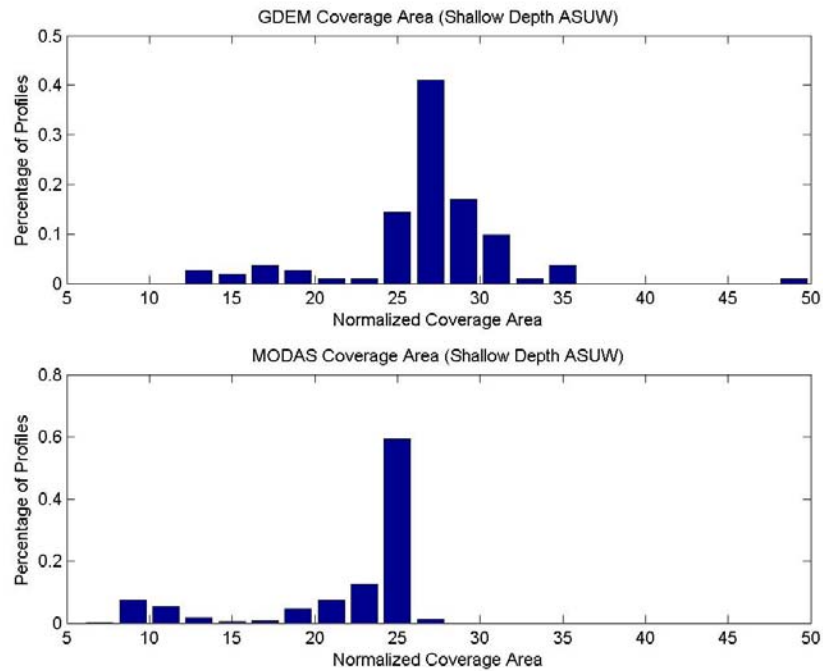


Figure 70. Shallow Depth ASUW Coverage Percentage Distribution

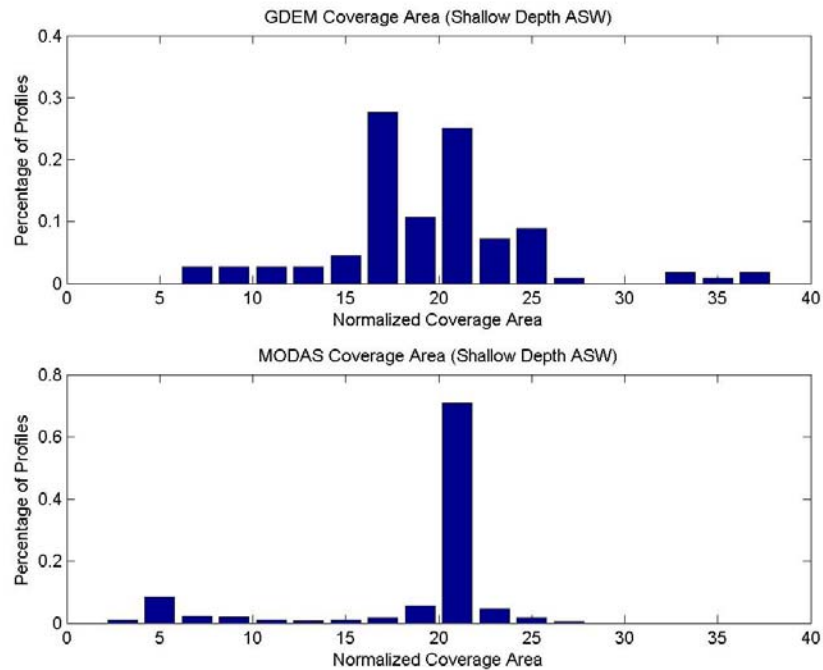


Figure 71. Shallow Depth ASW Coverage Percentage Distribution

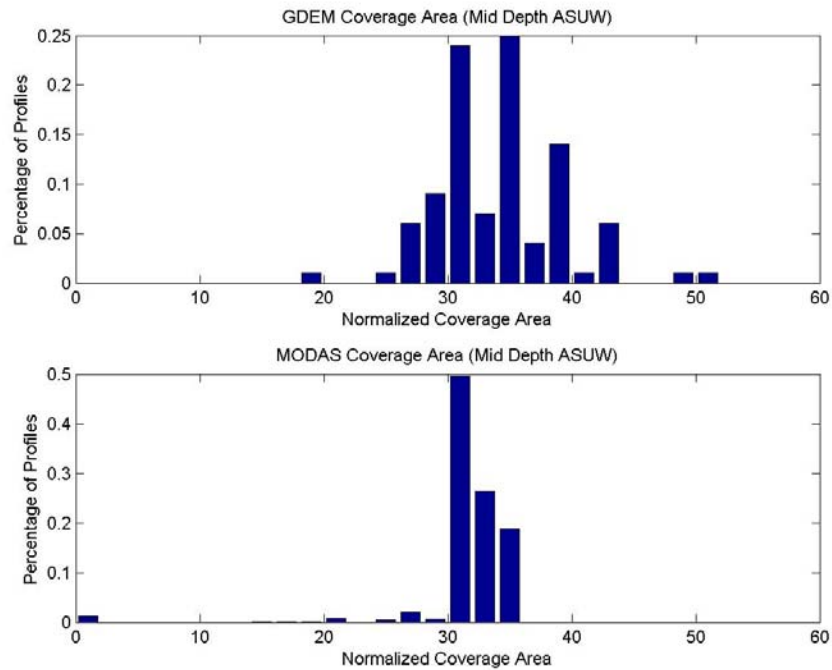


Figure 72. Mid Depth ASUW Coverage Percentage Distribution

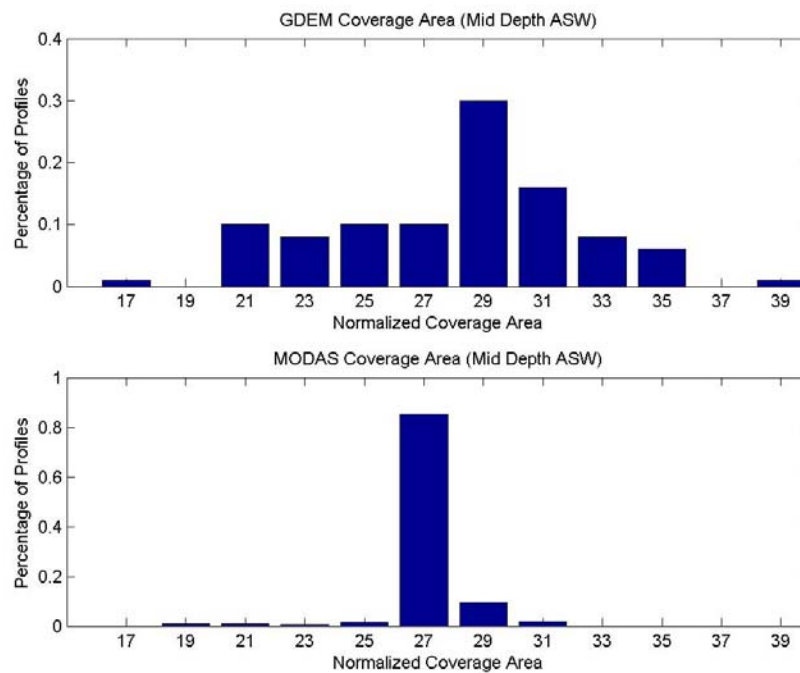


Figure 73. Mid Depth ASW Coverage Percentage Distribution

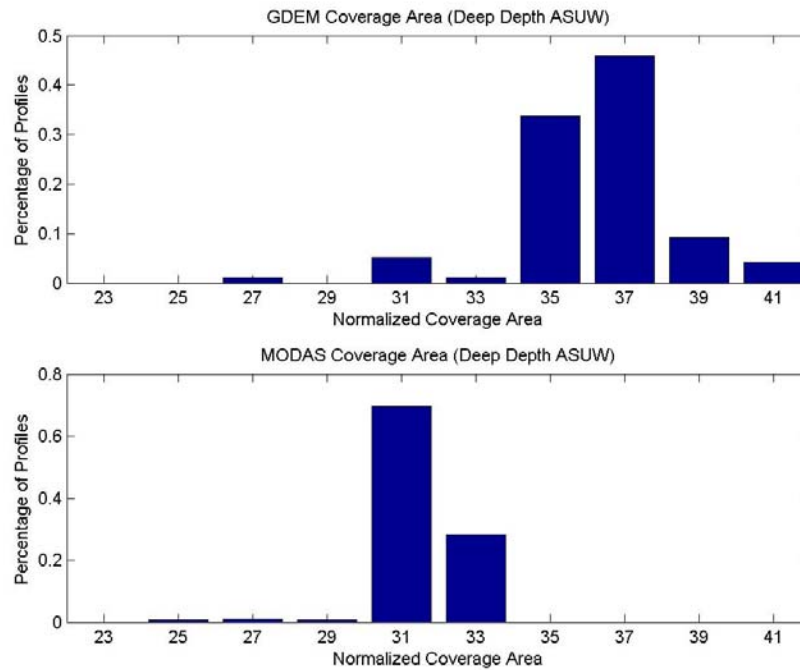


Figure 74. Deep Depth ASUW Coverage Percentage Distribution

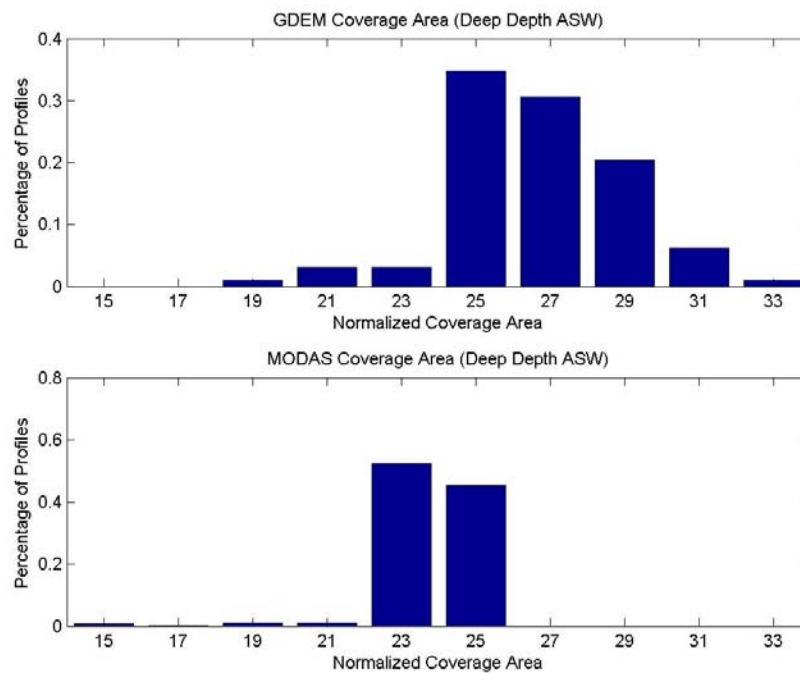


Figure 75. Deep Depth ASW Coverage Percentage Distribution

THIS PAGE INTENTIONALLY LEFT BLANK

LIST OF REFERENCES

- Fox, Daniel. “Modular Ocean Data Assimilation System.” [<http://7230.nrlssc.navy.mil/modas/>]. June 2003.
- Fox, D.N., W.J Teague, and C.N Barron, The Modular Ocean Data Assimilation System (MODAS). Journal of Atmospheric and Oceanic Technology, 19, 240-252, 2002.
- Jacobs, G.A., C.N. Barron, M.R. Carnes, D.N. Fox, H.E. Hurlburt, P. Pistek, R.C. Rhodes, and W.J. Teague, Naval Research Laboratory Report NRL/FR/7320-99-9696, Navy Altimeter Data Requirements, 1999.
- Naval Undersea Warfare Center, Acoustic Presetting Status, Power Point view graphs, 2002.
- Teague, W.J., M.J. Carron, and P.J. Hogan, A Comparison Between the Generalized Digital Environmental Model and Levitus Climatologies. Journal of Geophysical Research, 95, 7167-7183, 1990..

THIS PAGE INTENTIONALLY LEFT BLANK

INITIAL DISTRIBUTION LIST

1. Defense Technical Information Center
Ft. Belvoir, Virginia
2. Dudley Knox Library
Naval Postgraduate School
Monterey, California
3. Dr. Brian Almquist
Office of Naval Research
Arlington, VA
4. Dr. Charlie Barron
Naval Research Laboratory
Stennis Space Center, MS
5. Dr. Daniel Fox
Naval Research Laboratory
Stennis Space Center, MS
6. PMW 150
SPAWAR
San Diego, CA
7. Dr. Steve Haeger
Naval Oceanographic Office
Stennis Space Center, MS
8. Mr. Bruce Northridge
CNMOC
Stennis Space Center, MS
9. RADM John Pearson
Chair of Mine Warfare
Naval Postgraduate School
Monterey, CA
10. Oceanography Chair
Naval Postgraduate School
Monterey, CA
11. Dr. David Cwalina
Naval Undersea Warfare Center
Newport, RI

12. Mr. Roberts Rhodes
Naval Research Laboratory
Stennis Space Center, MS
13. Dr. Greg Jacobs
Naval Research Laboratory
Stennis Space Center, MS